Received: 8 May 2018 | Revised: 15 June 2020 | Accepted: 18 June 2020

DOI: 10.1111/cmi.13243

WILEY

RESEARCH ARTICLE

EIF2α phosphorylation is regulated in intracellular amastigotes for the generation of infective *Trypanosoma cruzi* trypomastigote forms

Fabricio Castro Machado[1] | Paula Bittencourt-Cunha[1] | Amaranta Muniz Malvezzi[1] | Mirella Arico[1] | Santiago Radio[2,3] | Pablo Smircich[2,3] | Martin Zoltner[4] | Mark C. Field[5,6] | Sergio Schenkman[1]

[1]Departmento de Microbiologia, Imunologia e Parasitologia, Escola Paulista de Medicina, Universidade Federal de São Paulo, São Paulo, Brazil

[2]Department of Genomics, Instituto de Investigaciones Biológicas Clemente Estable, Ministerio de Educación y Cultura, Montevideo, Uruguay

[3]Laboratory of Molecular Interactions, Facultad de Ciencias, Universidad de la República, Montevideo, Uruguay

[4]Drug Discovery and Evaluation, Centre for Research of Pathogenicity and Virulence of Parasites, Charles University, Prague, Czech Republic

[5]Division of Biological Chemistry and Drug Discovery, University of Dundee, Dundee, UK

[6]Institute of Parasitology, Czech Academy of Sciences, Prague, Czech Republic

Correspondence
Sergio Schenkman, Departmento de Microbiologia, Imunologia e Parasitologia, Escola Paulista de Medicina, Universidade Federal de São Paulo, R. Pedro de Toledo 669 L6A, São Paulo SP, 04039-032, Brazil.
Email: sschenkman@unifesp.br

Funding information
Conselho Nacional de Desenvolvimento Científico e Tecnológico, Grant/Award Numbers: 445655/2014-3, INCT-Vaccine; Fundação de Amparo à Pesquisa do Estado de São Paulo, Grant/Award Numbers: 2014/01577-2, 2015/20031-0, 2017/02496-4

Abstract

Trypanosomatids regulate gene expression mainly at the post-transcriptional level through processing, exporting and stabilising mRNA and control of translation. In most eukaryotes, protein synthesis is regulated by phosphorylation of eukaryotic initiation factor 2 (eIF2) at serine 51. Phosphorylation halts overall translation by decreasing availability of initiator $tRNA^{met}$ to form translating ribosomes. In trypanosomatids, the *N*-terminus of eIF2α is extended with threonine 169 the homologous phosphorylated residue. Here, we evaluated whether eIF2α phosphorylation varies during the *Trypanosoma cruzi* life cycle, the etiological agent of Chagas' disease. Total levels of eIF2α are diminished in infective and non-replicative trypomastigotes compared with proliferative forms from the intestine of the insect vector or amastigotes from mammalian cells, consistent with decreased protein synthesis reported in infective forms. eIF2α phosphorylation increases in proliferative intracellular forms prior to differentiation into trypomastigotes. Parasites overexpressing $eIF2\alpha^{T169A}$ or with an endogenous CRISPR/Cas9-generated $eIF2\alpha^{T169A}$ mutation were created and analysis revealed alterations to the proteome, largely unrelated to the presence of μORF in epimastigotes. $eIF2\alpha^{T169A}$ mutant parasites produced fewer trypomastigotes with lower infectivity than wild type, with increased levels of sialylated mucins and oligomannose glycoproteins, and decreased galactofuranose epitopes and the surface protease GP63 on the cell surface. We conclude that eIF2α expression and phosphorylation levels affect proteins relevant for intracellular progression of *T. cruzi*.

KEYWORDS
differentiation, eIF2, phosphorylation, translation, *Trypanosoma cruzi*, virulence

1 | INTRODUCTION

Changes to temperature, pH, oxidative state, nutrient and ionic concentrations are all environmental challenges that *Trypanosoma cruzi* parasites encounter during their life cycle (Souza, 2009).

Fabricio Castro Machado, Paula Bittencourt-Cunha, and Amaranta Muniz Malvezzi contributed equally to this study.

Consequently, the parasite changes gene expression, metabolism and morphology to adapt to these conditions (Piacenza, Alvarez, Peluffo, & Radi, 2009; Goldenberg & Avila, 2011; Moretti & Schenkman, 2013; Amorim et al., 2017). How parasites sense environmental conditions, and which signals initiate alterations to gene expression remain poorly characterised. Few gene-specific transcription promoters are present in trypanosomes with the exception of the spliced leader, ribosomal RNA promoters and expression site promotors in *Trypanosoma brucei* (Haile & Papadopoulou, 2007; Cribb, Esteban, Trochine, Girardini, & Serra, 2010; Martinez-Calvillo, Vizuet-de-Rueda, Florencio-Martinez, Manning-Cela, & Figueroa-Angulo, 2010). Transcription by RNA polymerase II produces long transcripts of non-related genes, which are processed by *trans*-splicing and polyadenylation to generate mature mRNAs prior to export to the cytoplasm (Palenchar & Bellofatto, 2006; Zinoviev & Shapira, 2012; Clayton, 2019). Furthermore, gene expression continues to be regulated within the cytoplasm by selection of which mRNAs are stored, degraded or translated in each specific life stage (Lahav et al., 2011; Kramer, 2012; Schwede, Kramer, & Carrington, 2012; Fritz et al., 2015).

Differentiation of *T. cruzi* proliferative forms, either in the insect vector (epimastigotes) or inside mammalian cells (amastigotes), into non-proliferative infective trypomastigotes is accompanied by global decreases in transcription and translation (Elias, Marques-Porto, Freymuller, & Schenkman, 2001; Ferreira, Dossin Fde, Ramos, Freymuller, & Schenkman, 2008; Smircich et al., 2015). Recent reports attribute key roles for RNA-binding proteins (RBPs) in regulating mRNA availability for translation through storage and degradation processes in trypanosomes (Cassola, 2011; Das et al., 2012; Guerra-Slompo et al., 2012; Kolev, Ramey-Butler, Cross, Ullu, & Tschudi, 2012; Perez-Diaz et al., 2012; Umaer & Williams, 2015; Belew et al., 2017; Mugo & Clayton, 2017). It is assumed that RBPs bind to specific mRNA regions to promote engagement with the translation machinery or the multiple classes of RNA granules (Markmiller et al., 2018). Phosphorylation of eIF4 paralogs has been suggested as a regulatory mechanism governing targeting of distinct mRNA species (Pereira et al., 2013), while translation also correlates with phosphorylation levels of eIF2, probably allowing response to altered conditions during life stage transition (Kramer et al., 2008; Chow, Cloutier, Dumas, Chou, & Papadopoulou, 2011; Tonelli, Augusto, Castilho, & Schenkman, 2011; Cloutier et al., 2012; Avila et al., 2016).

eIF2 is a heterotrimer (α, β and γ) and in *T. cruzi*, the α-subunit is phosphorylated at threonine 169, which is homologous to a highly conserved serine at position 51 in most eukaryotes due to the presence of an *N*-terminal extension (Moraes et al., 2007). eIF2α phosphorylation inhibits GDP to GTP exchange promoted by the eIF2B guanine exchange factor (GEF), decreasing the availability of the translation complex $eIF2^{GTP}$ and initiator methionine tRNA, $tRNA^{Met}$ (Pavitt, Ramaiah, Kimball, & Hinnebusch, 1998; Krishnamoorthy, Pavitt, Zhang, Dever, & Hinnebusch, 2001; Kashiwagi et al., 2016; Bogorad, Lin, & Marintchev, 2017). Decreased levels of $eIF2^{GTP}$-$tRNA^{Met}$ reduce global protein synthesis while allowing translation of mRNAs containing multiple initiation sites or μORFs. These mRNAs encode transcription factors that regulate genes involved in remediating cellular stresses (Pavitt et al., 1998; Hinnebusch, 2000; Sonenberg & Hinnebusch, 2009; Palam, Baird, & Wek, 2011; Baird & Wek, 2012). In mammalian cells, μORF-encoded proteins include transcriptional regulators activating transcription factor 4 (ATF4), C/EBP homologous protein (CHOP) and a regulatory subunit of protein phosphatase 1, which can dephosphorylate eIF2α (Sonenberg & Hinnebusch, 2009).

eIF2α phosphorylation at T169 in *T. cruzi* epimastigotes is induced by nutritional stress and mutation to alanine prevents full translation arrest impacting metacyclic differentiation (Tonelli et al., 2011). eIF2α phosphorylation also regulates protein synthesis in *Leishmania* (Chow et al., 2011). Nevertheless, the role of eIF2α availability and its phosphorylation on regulating translation remains largely uncharacterized in trypanosomes. Here, we evaluate eIF2α level, phosphorylation state and relevance to different stages of *T. cruzi*. eIF2α is relatively decreased in trypomastigote forms, compatible with a low translation activity but is increased in amastigotes prior to differentiation into infective forms. To demonstrate the importance of this phosphorylation, we overexpressed wild-type eIF2α and $eIF2\alpha^{T169A}$ mutants and observed a large decrease in infectivity. Furthermore, alterations to the surface proteome suggest specific changes to virulence-associated protein families, suggesting direct roles for eIF2α in modulation of infectivity.

2 | RESULTS

2.1 | EIF2α expression is decreased in non-proliferative T. cruzi life stages

To characterise alterations in eIF2α across multiple developmental stages of *T. cruzi*, western blotting was used with an antibody generated against bacterially expressed *T. cruzi* eIF2α. Ten micrograms of protein from soluble extracts obtained from replicative epimastigotes (Epi) and intracellular amastigotes (Ama) and non-proliferative but infective metacyclic-trypomastigotes (Meta) and tissue culture-derived trypomastigotes (Trypo) were subjected to electrophoresis and blotting (Figure 1a). Both Meta and Trypo possess reduced levels of eIF2α compared with proliferative forms (Figure 1b) and were specific as similar decreases were apparent relative to Hsp70 and BiP, cytosolic and ER chaperones respectively (Figure 1c,d). We also noticed diminished expression of eIF2α relative to eIF5A in metacyclic-trypomastigotes (Figure 1e), consistent with a specific decrease in proteins involved in translation recently described in metacyclics (Schuller, Wu, Dever, Buskirk, & Green, 2017). Therefore, we suggest that down-modulation of eIF2α expression in infective forms likely relates to diminished translational activity and may also reflect altered protein expression patterns in proliferating versus infective *T. cruzi* stages.

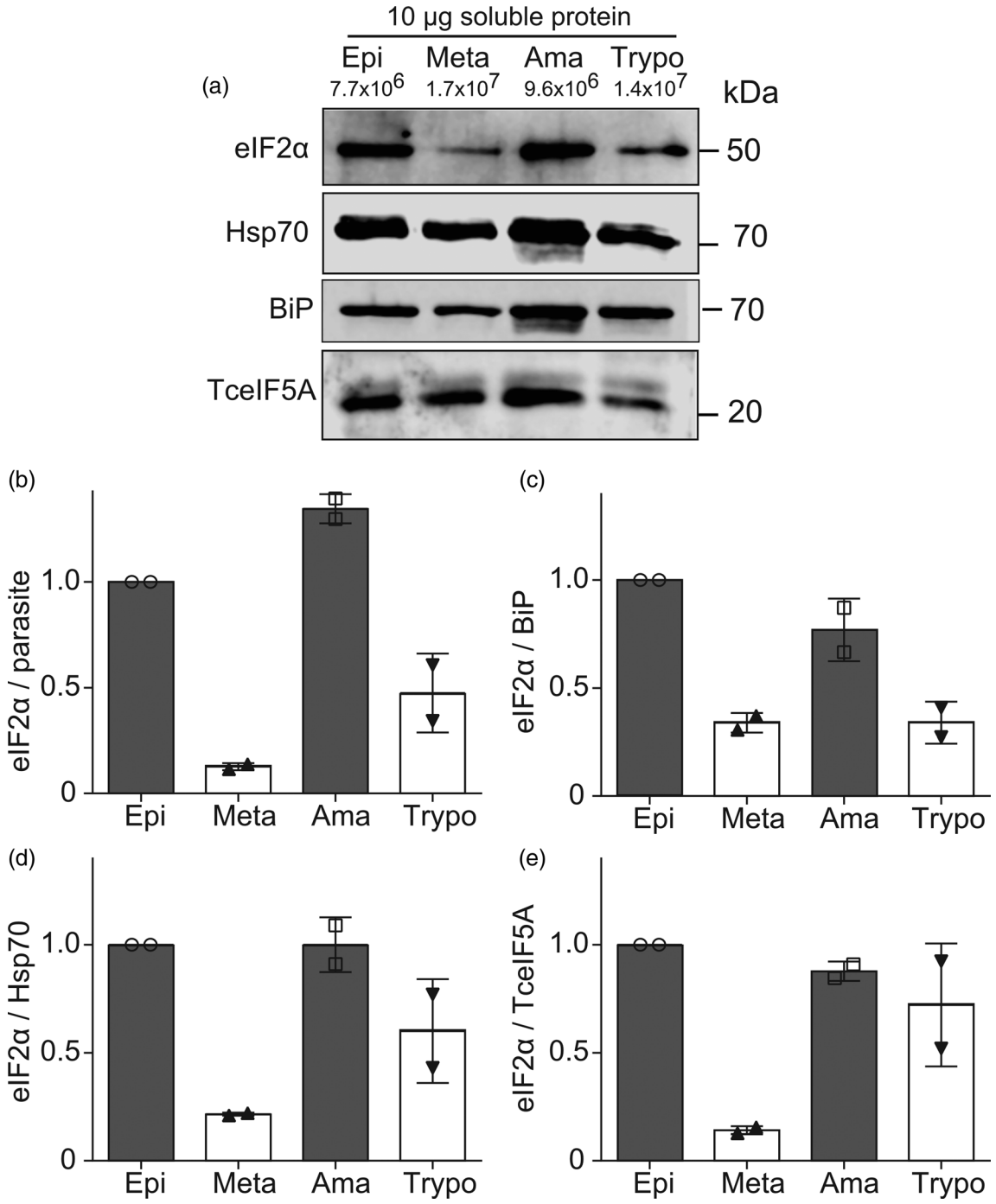

FIGURE 1 Reduced eIF2α expression in non-proliferative forms of *T. cruzi*. (a) Western blotting of soluble extracts containing 10 µg of protein per lane was obtained from the indicated amounts of epimastigotes (Epi), metacyclic-trypomastigotes (Meta), intracellular amastigotes (Ama) and tissue-cultured derived trypomastigotes (Trypo) forms. The membranes were probed with antibodies to eIF2α, Hsp70, BiP and Eif5a. means of eIF2α signal relative to parasites numbers (b), BiP (c) Hsp70 (d) and eIF5A (e) were calculated from duplicate experiments and the symbols indicate the values obtained in each experiment. Considering the eIF2α versus all other proteins simultaneously, a significant difference was observed ($p = .0278$, $n = 6$) using Welch two tailed *t*-test

2.2 | eIF2α phosphorylation increases in the intracellular replication cycle prior to differentiation into trypomastigotes

Trypomastigotes enter mammalian cells by forming a parasitophorous vacuole, and from 4 to 12 hr, depending on the host cell and parasite strain, most parasites exit the vacuole and transform into amastigotes (Rubin-de-Celis, Uemura, Yoshida, & Schenkman, 2006). Amastigotes start dividing in the host cell cytosol 24 hr after invasion and in about 4 days occupy the entire cytosol and transform into trypomastigotes, which are released by host cell rupture, usually after 5 days of infection. To further investigate how and whether a decrease in translation

in trypomastigotes is related to eIF2α phosphorylation, we examined intracellular amastigotes collected 2, 3 and 4 days after infection by western blotting with an antibody against phosphorylated T169 of eIF2α^{T169P} relative to total eIF2α and Hsp70. eIF2α^{T169P} increased from 72 hr, peaking at 96 hr after infection, the last day before differentiation into trypomastigotes (Figure 2a). Quantitative analysis confirmed these observations and indicate that released trypomastigotes have decreased eIF2α^{T169P} relative to both total eIF2α (Figure 2b) and Hsp70 (Figure 2c) 3 and 4 days post-infection. Therefore, increased levels of eIF2α^{T169P} occur in amastigotes, probably related to differentiation, but concomitant with decreased total eIF2α and translation.

2.3 | Generation of parasite lines overexpressing non-phosphorylatable eIF2α and parasites

eIF2α contains an *N*-terminal extension adding 118 amino acids in *T. cruzi*, such that T169 corresponds to S51 in other eukaryotes (Figure 3a) and is involved in regulation of global protein translation in *T. cruzi* epimastigotes (Tonelli et al., 2011). To determine whether T169 phosphorylation also affects control of protein synthesis and differentiation of *T. cruzi*, and specifically in mammalian stages of the parasite, we overexpressed eIF2α in a similar approach as used by Tonelli et al. (2011) but without an epitope tag. Four different epimastigote lines were produced: a wild-type version (WT), a version with serine 43 mutated to alanine (S43A), a version with T169 mutated to alanine (T169A) and a version with both mutations (S43A/T169A). A control containing the green fluorescent protein (GFP) expression fused to histone H2B was also prepared as described previously (Ramirez, Yamauchi, de Freitas Jr., Uemura, & Schenkman, 2000). The epimastigote lines had over threefold overexpression of eIF2α, which was stable at least until 21 days without drug selection (Figure S1a,b). Interestingly, cells from these lines were smaller (Figure S1c,e) and importantly global translation was not completely abrogated in comparison with the wild-type line incubated in starvation conditions (Figure S2a), as shown previously (Tonelli et al., 2011).

We also generated parasites with the eIF2α^{T169A} mutation using CRISPR/Cas9 to specifically mutate both endogenous loci. Cells expressing a Cas9-GFP fusion were transfected with an appropriate guide RNA and donor oligonucleotide in which the T169A mutation and a BssHII site were inserted. This was prepared by targeting the single guide RNA to the eIF2α ORF, just after the T169 coding sequence (AGG). The repairing was made using a donor containing the sequence GCGCGC (BssHII site) to code for the amino acids A and R. After two rounds of transfection, more than 95% of the parasites contained the insertion as evaluated by PCR and BssHII restriction (Figure 3b) and the correct mutation validated by sequencing. The parasites were cloned by limiting dilution and a clone displaying full BssHII digestion selected. Digestion with BssHII of the PCR product corresponding to the eIF2α gene showed full digestion, confirming the absence of parasites without mutation (Figure 3b). Moreover, lysates from the eIF2α^{T169A} clone were not recognised by anti-phospho-eIF2α antibodies, even after nutritional stress (TAU), a condition that increases phosphorylation of eIF2α (Figure 3c). Importantly, protein levels of eIF2α were similar in both cell types and we always detected some eIF2α phosphorylation in wild-type parasites. The eIF2α^{T169A} overexpression parasites also showed less efficient translation arrest compared with the eIF2α^{T169A} Cas9 strain as was the case of the overexpressors containing the mutation (Figure S2b). The epimastigote lines were also used to obtain metacyclic-trypomastigotes, which infected mammalian cells and produced new rounds of cell-derived trypomastigotes. In the eIF2α^{T169A} overexpressing lines, these trypomastigotes continued to exhibit higher levels of eIF2α in relation to Hsp70 and aldolase compared with wild-type parasites indicating that the overexpression phenotype remained stable despite differentiation (Figure S1e,f).

2.4 | Absence of eIF2α phosphorylation affects protein expression in T. cruzi

Epimastigotes and metacyclic-trypomastigotes derived from eIF2α^{T169A} overexpressor lines expressed increased amounts of the *trans*-sialidase family members gp82 and gp90 (Figure S3a), both of which are preferentially expressed in metacyclic-trypomastigotes (Yoshida, Blanco, Araguth, Russo, & Gonzalez, 1990; Araya, Cano, Yoshida, & Da Silveira, 1994). Quantitative analysis indicated a threefold increase in gp90 expression for eIF2α^{T169A} and eIF2α^{S43AT169A} cells compared with GFP, WT or eIF2α^{S43A} parasites (Figure S3b). No differences were observed for antibodies that recognised mucin-like glycoprotein in these epimastigotes. In contrast eIF2α^{T169A}, parasites obtained by CRISPR did not express gp90 in epimastigotes (Figure S3c), indicating that overexpression of eIF2α^{T169A} differently affected parasites compared with mutation and retention of endogenous expression levels.

To characterise these changes in more detail CRISPR/Cas9 parental and eIF2α^{T169A}, mutant cells were analysed by LC-MSMS. A total of 4,301 protein groups were identified, representing approximately ~30% of the *T. cruzi* proteome (Table S2, protein groups). Considering only robust data, (applying a cut-off $-\log_{10}$ *p*-value >1; Table S2 increased and decreased Log *p* > 1, see methods) calculated using five control independent samples and four independent T169A samples (Table S2, summary), the abundance of 217 protein groups was decreased and the abundance of 205 was increased (Figure 3d). As *T. cruzi* genome annotation remains rather poor, we grouped these protein groups by function based on the possession of Interpro domains and similarities to annotation of syntenic genes in other trypanosomatids, mainly *T. brucei* (Figure 4 and Table S3). We found that the mutant had decreased levels of surface proteins, glycoprotein synthesis enzymes, redox enzymes, cell cycle control, cytoskeleton, several phosphatases, ADP-ribosylation and lipid metabolism. In contrast, absence of eIF2α phosphorylation produced cells with more proteins involved in amino-acid metabolism, several chaperones, chromatin structure and transcription. Furthermore, *trans*-sialidase gene family members are significantly enriched in the decreased

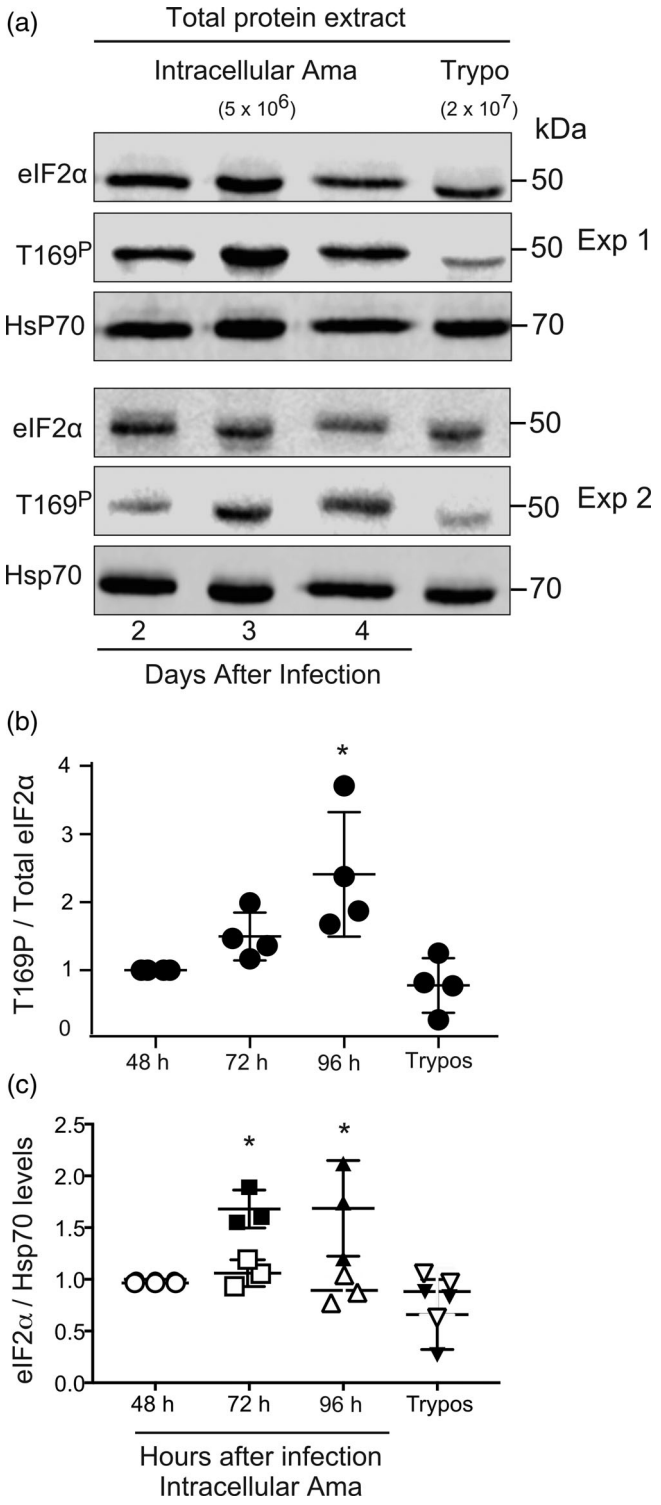

FIGURE 2 Kinetics of eIF2α phosphorylation during amastigote development. (a) Total cellular extracts obtained from 5×10^6 intracellular amastigotes collected 2, 3 or 4 days post-infection and from 2×10^7 trypomastigotes released in the supernatant (Trypos) were used in western blotting. The membranes were probed with antibodies to total eIF2α protein, antibodies to the phosphorylated form of eIF2α at threonine 169 ($T169^P$) and anti-Hsp70. Images from two independent experiments are shown (Exp 1 and Exp 2). (b) Pixel signal quantification of phosphorylated $T169^P$ relative to values obtained for total eIF2α normalised to the values at day 2 post-infection. (c) Values of total eIF2α (open symbols) and $T169^P$ (closed symbols) relative to Hsp70 levels. Values show points of the different experiments and mean ± standard deviation values of four independent experiments. The asterisk indicates $p < .05$ in relation to 2 days post-infection values calculated using two-way analysis of variance considering the means of individual experiments followed by Dunnett's correction

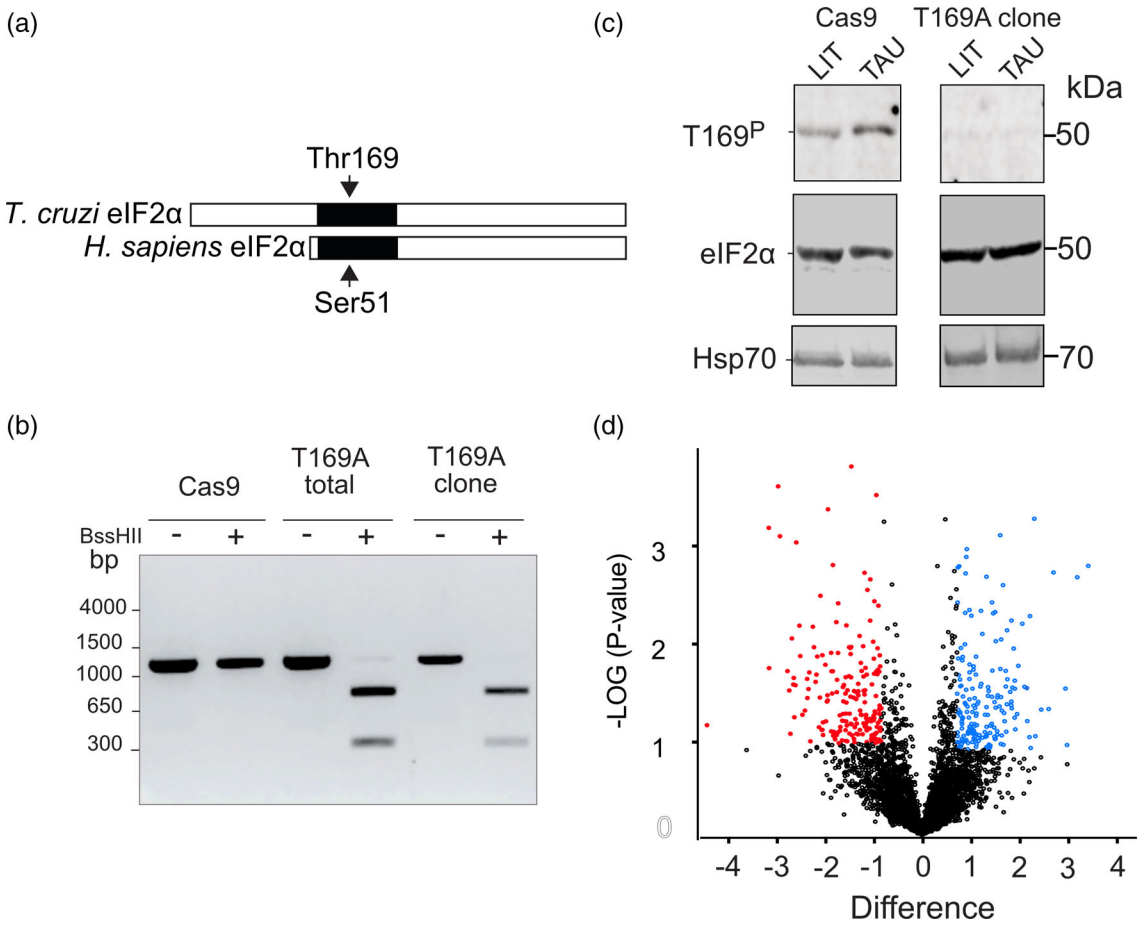

FIGURE 3 T169 mutation in eIF2α deregulates stage-specific expression. (a) Diagram comparing *T. cruzi* and human eIF2α. The arrows indicate the phosphorylation site at threonine 169 (T169) of *T. cruzi* eIF2α and serine 51 (S51) of the *Homo sapiens* eIF2α. The black boxes correspond to S1 domain, responsible for interaction with the ribosomes. (b) Agarose gel (0.8%) stained with ethidium bromide of the PCR product corresponding to a fragment of the eIF2α gene obtained from the indicated epimastigote lines, untreated (–) or treated (+) with BssHII enzyme. The size markers are indicated on the left side of the gel in base pairs (bp). (c) Western blotting of epimastigotes (~3×10^6 per lane) from the indicated lines pre-incubated for 6 hr in LIT medium or in TAU medium. The top panel corresponds to membranes incubated with antibodies to the phosphorylated eIF2α ($T169^P$) followed by mouse anti-eIF2α developed using IRDye680 and IRDye800 respectively. (d) Volcano plot showing the difference in expression of the mutant relative to control strains identified by mass spectrometry using five independent samples of controls and five independent samples of Cas9-T169A epimastigotes maintained in LIT medium. The samples were run on SDS-PAGE gels and analysed by LC MS/MS as described in Methods. The volcano plot shows the $-\log_{10}$-transfomed *t*-test *p*-value versus the *t*-test difference (difference between means) for each protein group. High confidence cohorts (with –log10 *t*-test *p*-values above 1) used in the enrichment analysis are in highlighted in colour

cohort (–log p > 0.5 cutoff) with an enrichment factor of 2.5 and a false discovery rate (FDR) < 2% (Table S4). It is also particularly relevant that the eIF2α kinase similar to PERK (TcK2) increased about seven times in the mutant cells, suggesting an adaptation by these mutants to rectify the decrease in phospho-$eIF2\alpha^{T169}$ by increased kinase activity. Protein biosynthesis and surface export pathways appear impacted and several activities related to transcription and chromatin state are affected.

As genes containing micro-open reading frames (μORF) are preferentially translated upon eIF2α phosphorylation (Andreev et al., 2015), we generated the 5′ untranslated regions and 3′UTR of the mRNAs of *T. cruzi* YC6 genome using the UTRme software, specifically developed for trypanosomatids (Radio, Fort, Garat, Sotelo-Silveira, & Smircich, 2018) (Table S4) and μORFs with repressive characteristics were annotated (see Materials and Methods section for details). When we selected the proteomic hits within high confidence prediction values ($-\log_{10}$ p-value >1), we found no correlation between the 5′ UTR length and increased protein expression (Figure S4a). Overlapping μORFs was slightly enriched in the down-regulated proteins cohort with an enrichment factor of 1.7 (FDR < 2%) (Table S4).

As the codon adaptation index (CAI) has been linked to protein levels in trypanosomes (Jeacock, Faria, & Horn, 2018), decreased eIF2α phosphorylation could affect less abundant proteins, that is, those with low MS/MS counts. Genes with high CAI are more expressed in epimastigotes (Figure S5a). However, abrogation of the

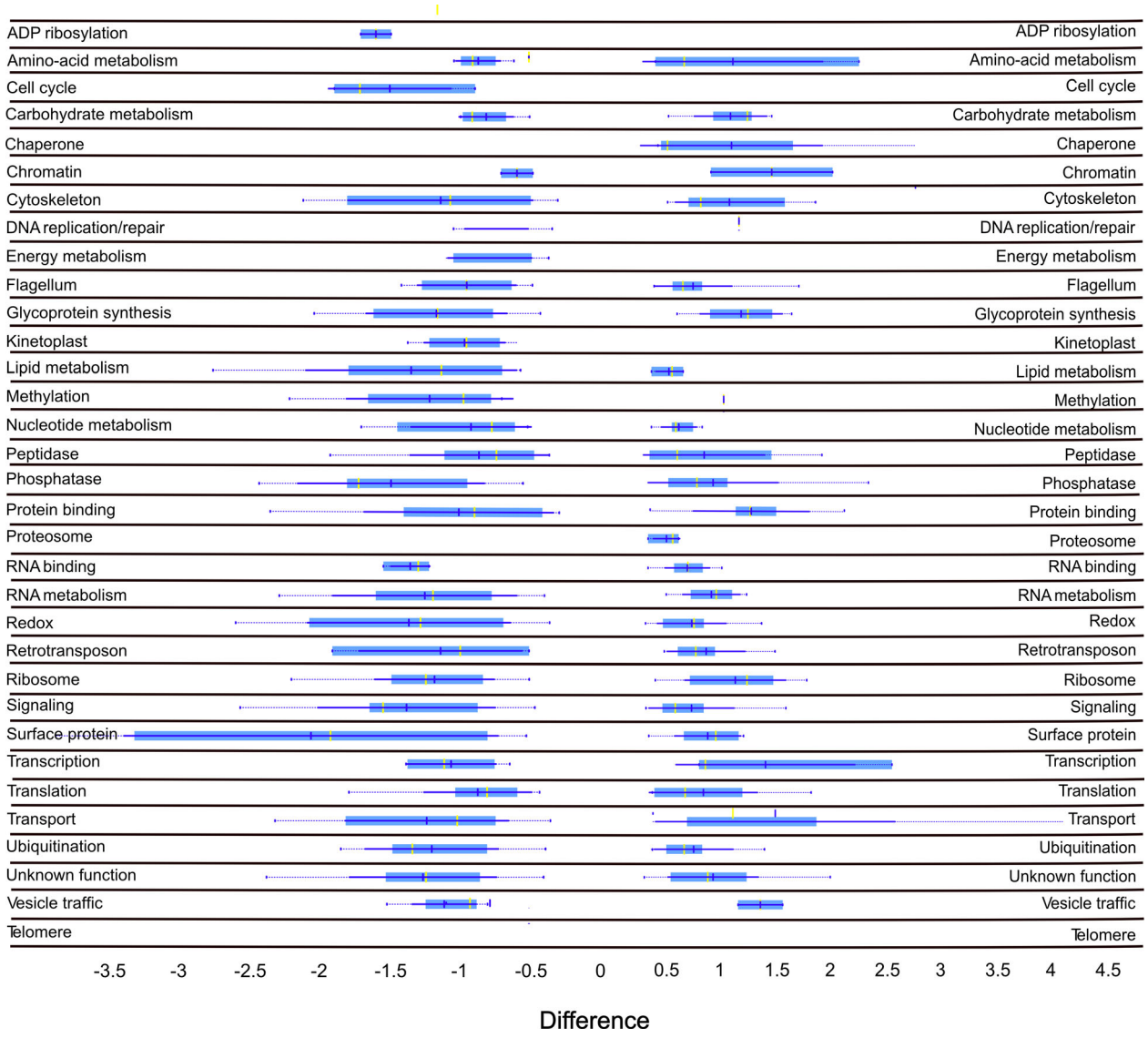

FIGURE 4 Unique gene types are decreased and increased in eIF2α mutated epimastigotes. Different functional categories were assigned to protein groups quantified by the MS/MS analysis and plotted against the *t*-test difference (considering the number of hits across the respective difference interval (Size of horizontal large blue bars). These functional categories were obtained by direct comparison with annotations for syntenic genes of other trypanosomatids and Interpro domains. The box plot was generated by the Orange3 software and the mean (yellow) and median values (blue vertical lines) estimated for each case. The thick blue line represents the limit of significant variations and the dotted line the observed end values

eIF2α phosphorylation showed no correlation with the cohorts of differentially expressed proteins (Figure S5b). The data of CAI for all CDS detected in *T. cruzi* are shown in Table S5.

2.5 | Impaired phosphorylation of eIF2α decreases parasite infectivity and replication in mammalian host cells

Next, we investigated the importance of eIF2α to mammalian cell and animal infectivity by using eIF2α mutant trypomastigotes. We used U-2 OS human osteosarcoma and LLC-MK2 epithelial kidney cells as in vitro infection models (Moon et al., 2014). Initially, we measured infection ratio, that is, number of infected relative to total cells, using different multiplicities of infection (MOI) of parental, eIF2α overexpressors and eIF2α^{T169A} mutants. eIF2α^{T169A} parasites had a significantly decreased infectivity compared with control parasites even at different MOI (Figure 5a). We detected a significant increase of amastigotes replication in cells overexpressing wild-type eIF2α compared with control cells. eIF2α^{T169A} overexpressor lines had a decreased proliferation rate (Figure 5b), which was clear in stained cultures (Figure S6a) and across different MOI (Figure S6b–d). Similar results were observed when infecting LLC-MK2 cells, showing a reduced number of intracellular amastigotes in cells infected with both eIF2α^{T169A} lineages (Figure 5c). A similar decrease in intracellular proliferation could be observed just after 2 and 3 days of infection

(Figure S6e,f respectively). Importantly, fewer trypomastigotes were released from LLC-MK2 cells infected with eIF2α^{T169A} mutants compared with control lines (Figure 5d), expected, due to their decreased invasion and/or growth rate.

We also examined the impact of eIF2α mutation by CRISPR/Cas9. Mutated epimastigotes differentiate less into metacyclic-trypomastigotes (Figure 5e) and trypomastigotes released from infected mammalian cells showed decreased invasion of U-2 OS cells (Figure 5f). Furthermore, the mutant amastigotes proliferated more slowly and less trypomastigotes were released from infected (Figure 5g,h), confirming that the absence of eIF2α phosphorylation contributed to compromised infectivity in an in vitro model.

2.6 | Parasites containing non-phosphorylatable eIF2α are less virulent in mice

Overexpressor eIF2α^{T169A} trypomastigotes yield reduced levels of blood parasitemia in mice compared with parental or to parasites overexpressing wild-type eIF2α (WT) (Figure 6a). This decrease was

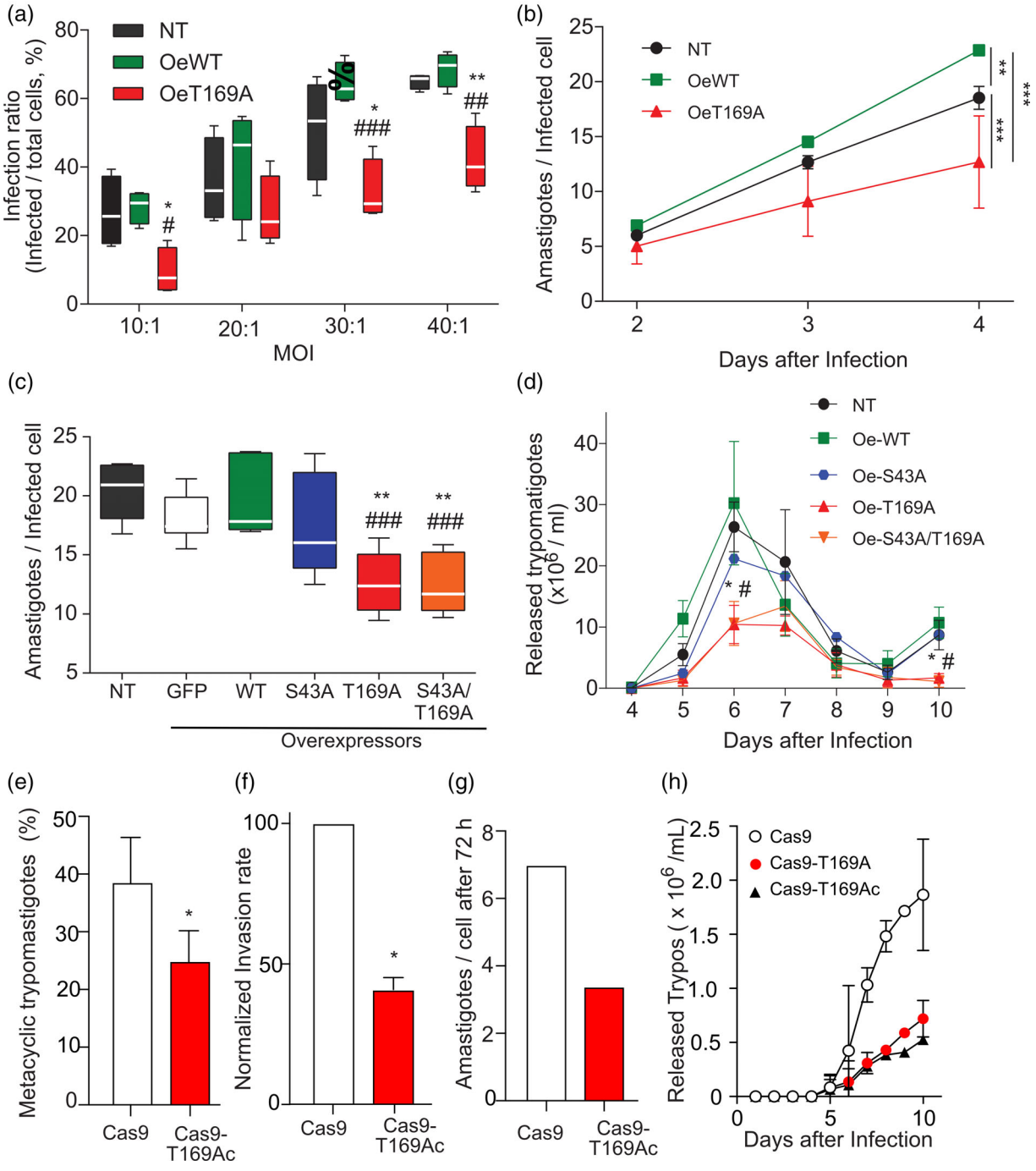

FIGURE 5 Legend on next page.

even more pronounced in the second peak of parasitemia, indicating that the animals were more efficiently controlling the infection caused by eIF2α^{T169A} parasites. As animals survived the acute phase, to determine whether they remained infected, mice were immunosuppressed with cyclophosphamide. Parasites appeared later, and with lower parasitemia in the blood of mice when infected with eIF2α^{T169A} overexpressing parasites compared with the control lines (Figure S7a). Indeed, this resulted in delayed mortality in the animals infected with eIF2α^{T169A} overexpressors (Figure 7b). Together, these results indicate that overexpression of non-phosphorylatable eIF2α^{T169A} modulates *T. cruzi* infectivity.

2.7 | Mutant trypomastigotes have a distinct surface composition

As many surface molecules are known to be important for infection, we collected trypomastigotes released on the first and second day from infected cells and compared the major surface proteins between mutant and control parasites. Released parasites were fixed in *p*-formaldehyde and stained with monoclonal mAb 3C9, which recognises sialylated mucin-like glycoproteins and with concanavalin A, which recognises surface glycoproteins containing *N*-linked oligomannose chains, found in the large family of *trans*-sialidase proteins (Mucci, Lantos, Buscaglia, Leguizamon, & Campetella, 2016). Mutated parasites express higher amounts of both surface markers compared with control parasites (Figure 7a–d). In contrast, galactofuranose epitopes in glycosyl phosphatidylinositol (GPI) glycolypids recognised by mAb Mest-1 (Suzuki, Toledo, Takahashi, & Straus, 1997), found important for *Leishmania* invasion (Suzuki, Tanaka, Toledo, Takahashi, & Straus, 2002), were less exposed (Figure 7e,d). Mutated parasites also presented decreased amounts of the surface protease metalloprotease GP63 (Cuevas, Cazzulo, & Sanchez, 2003; Kulkarni, Olson, Engman, & McGwire, 2009) as detected by zymogram analysis, indicating significant changes on the parasite surface.

3 | DISCUSSION

Here, we evaluated the expression and phosphorylation state of *T. cruzi* eIF2α during all phases of the parasite life cycle, a key regulator of the translational apparatus. Total protein levels of eIF2α decreased in infective and non-proliferative trypomastigotes compared with both proliferative epimastigotes and amastigotes, whereas phosphorylated eIF2α increased during amastigote infection prior to the generation of trypomastigotes. When non-phosphorylatable eIF2α was overexpressed or endogenous eIF2α was replaced by the same mutated form parasites differentiate less efficiently and have lower infectivity. These changes occurred in parallel with alterations in protein expression, indicating a key role for eIF2α phosphorylation in life cycle progression as well as implicating the impacted proteins as players in this process.

Reduced eIF2α levels in trypomastigotes are compatible with the previous studies showing decreased translation in infective forms (Avila et al., 2003; Smircich et al., 2015), in parallel to a general

FIGURE 5 Non-phosphorylatable overexpression of eIF2α impairs invasion, amastigote replication and trypomastigote release. (a) The infection ratio was calculated based on the number of infected cells per total number of U-2 OS upon incubation with the indicated trypomastigote lines [(non-transfected, NT, black boxes); WT (green boxes) and T169A (red boxes)] overexpressors for 2 hr at different multiplicity of infection (MOI). The cells were washed and fixed after 3 days to allow better visualisation by the HCA method. The values are means (white traces), 25 and 75% percentiles (coloured boxes) and min and max values (deviation lines) of four independent experiments, each one measured in triplicate. The asterisk indicates $p < .05$ and ** $p < .01$ calculated using the two-way analysis of variance (ANOVA) in relation to NT parasites. ## indicates $p < .01$ and ### $p < .001$ also calculated by two-way ANOVA, using Tukey test correction, in relation to WT overexpressors. (b) HCA of intracellular amastigotes multiplication plotted as the number of amastigotes per infected U-2 OS cells 2, 3 and 4 days after infection with trypomastigotes (MOI = 40) of the indicated lineages. The values are means ± standard deviation of three independent experiments and the asterisk indicates $p < .05$, ** indicates $p < .01$ and *** $p < .001$ calculated using the two-way ANOVA, following Tukey test correction, at the third and fourth day of replication. (c) The graph shows the number of amastigotes present in each cell calculated from 100 infected LLC-MK2 cells determined at 4 days after infection with the indicated Trypo lineages (MOI = 10). The values were determined by optical microscopy after Giemsa staining, as described in Methods. The values are represented as in (a) and the asterisk indicates $p < .05$ and ** $p < .01$, both calculated using the one-way ANOVA considering the relation with NT parasites. # indicates $p < .05$, ## indicates $p < .01$ and ### indicates $p < .001$ calculated using the one-way ANOVA in relation to WT overexpressors. (d) LLC-MK2 cells were infected with the same number of trypomastigotes of each indicated cell lineages and the parasites released every day on the supernatant was assessed by counting by using a Neubauer chamber from 4 to 10 days after infection. The values are means ± standard deviation of three independent experiments and the differences are indicate with * ($p < .05$) in relation to NT parasites and # ($p < .05$) in relation to WT overexpressors, both calculated using Student's *t* test. (e) Metacyclic-trypomastigotes observed 7 days after the inoculation of exponentially growing epimastigotes (1×10^7/ml) in Grace's medium containing 10% FBS (initial concentration of epimastigotes was 3×10^7/ml. (f) Trypomastigotes (1×10^6/ml in 1 ml were added to U-2 OS (MOI-10) in 24-well plates containing glass coverslips. After 2 hr at 37°C, the parasites were removed, and the number of internalised parasites in duplicates was counted after Giemsa staining using two wells for each condition. In another set, the cells were further incubated in DMEM-10% FBS and stained after 72 hr (g). Numbers in E to G are mean and ± standard deviation of three independent experiments. The asterisk shows $p < .05$ using Student's *t* test. (h) LLC-MK2 cells (5×10^5) in 75 cm^2 were infected with trypomastigotes (5×10^6 – MOI = 10) for 24 hr. The parasites were replaced by fresh medium. The amount of released trypomastigotes of each line was then counted in the culture supernatant and the values shown are cumulative numbers of released parasites

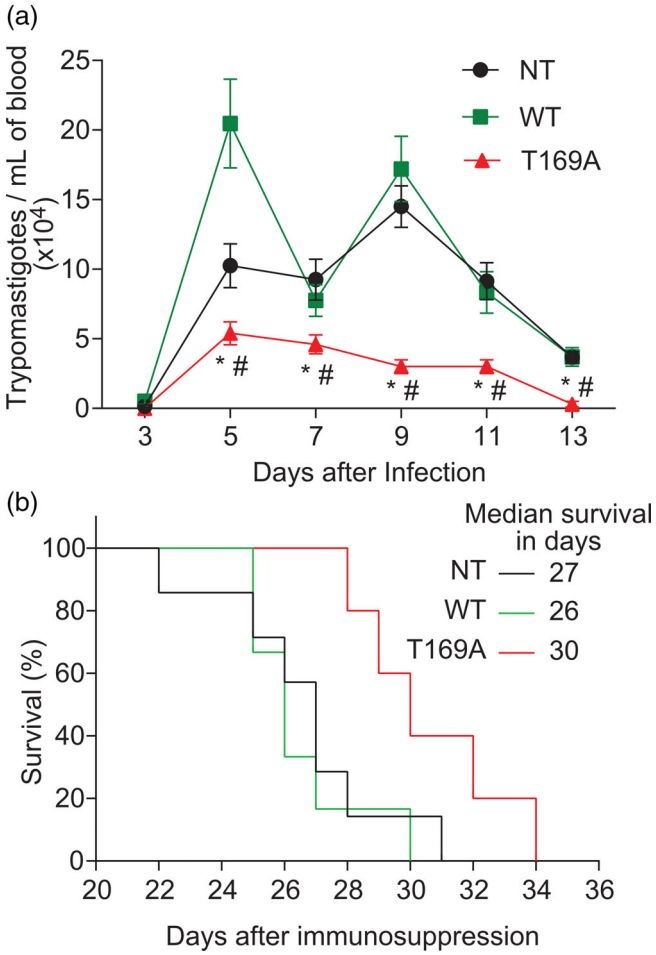

FIGURE 6 EIF2α phosphorylation affects infectivity in mice. (a) Mice were intraperitoneally infected with trypomastigotes of the indicated overexpressor lines and the number of parasites in the blood was followed as described in Methods. The plotted values are means ± standard error of two independent experiments using 10 mice for each group. The asterisk indicates $p < .05$ in relation to NT parasites and # $p < .05$ in relation to WT overexpressors, both calculated using Student's *t* test. (b) Forty days after infection, mice started to be immunosuppressed with cyclophosphamide, as described in Methods. The plot shows the days after immunosuppression and the survival was followed for NT ($n = 7$), WT overexpressors ($n = 6$) and T169A overexpressors ($n = 5$) infected mice showing different survival medians for each lineage

transcriptional reduction (Elias et al., 2001). As eIF2α phosphorylation is increased in intracellular amastigotes, this event could trigger translational decrease and induce differentiation into trypomastigotes, as observed in the transformation of epimastigotes to metacyclic-trypomastigotes (Tonelli et al., 2011). A similar mechanism is triggered for *Leishmania* when parasites infect macrophages and transform into amastigotes (Cloutier et al., 2012), but is in contrast to *T. brucei* in which the equivalent eIF2α mutation does not prevent differentiation into stumpy forms (Avila et al., 2016), a form with reduced translation levels (Brecht & Parsons, 1998). *Toxoplasma gondii* elevated levels of phospho-eIF2α are found in latent bradyzoites, the non or slow replicative form (Joyce, Queener, Wek, & Sullivan Jr., 2010). Therefore, control of translational arrest likely relies on distinct mechanisms in different lineages.

The pattern of protein expression in epimastigotes growing exponentially in rich medium is significantly altered when eIF2α phosphorylation is blocked. Under these conditions, eIF2α phosphorylation is present and suggests that translational initiation is constantly modulated in these cells. The decrease of surface protein expression, enzymes involved in maintaining redox homeostasis and control of cell cycle, likely explain both decreased differentiation and infectivity. eIF2α phosphorylation clearly alters the expression of specific trypomastigotes factors, and these likely include *trans*-sialidases, expressed in the final days of intracellular replication and prior to appearance of trypomastigotes (Frevert, Schenkman, & Nussenzweig, 1992; Abuin, Freitas, Colli, Alves, & Schenkman, 1999). The importance of precise regulation of protein expression at this point in the life cycle has been noted in the highly attenuated CL-14 clone of *T. cruzi*, which is significantly compromised in development of trypomastigotes (Belew et al., 2017). Reduced levels of enzymes such as peroxidases and oxidoreductases could also impair parasite fitness in mammalian cells as both invasion and proliferation are largely diminished.

We did not observe correlations with predicted 5′UTR length and the variation of protein levels in exponentially growing epimastigotes. Also, there was no strong correlation between the presence of μORFs and proteins down-regulated in epimastigotes, which, based on other studies, would be expected as a consequence of eIF2α phosphorylation. However, a slight overrepresentation of overlapping μORFs was indeed observed within the cohort of decreased proteins in eIF2α T169A mutant. This type of sequence has been suggested to exert a significant repression in translation efficiency of the main CDS in *T. cruzi* (Radio, Garat, Sotelo-Silveira, & Smircich, 2020). Interestingly, TcMucII, surface protease GP63 and the UDP-ß-galacofuranosyltransferase surface proteins related to virulence in trypomastigotes were shown to contain μORF (Figure S4c) and were found decreased in trypomastigotes. The decreased amounts of ß-galactofuranose in glycolipids and GP63 protease could explain the decreased invasion capacity of the eIF2α mutations (Suzuki et al., 2002; Kulkarni et al., 2009). Also, the high recognition levels of sialylated mucins and concanavalin A in mutated parasites could, therefore, reflect their differential expression. One possibility is that translation arrest could potentiate their expression by excluding them from RNA stress granules (Aulas et al., 2017). The presence of specific RNA binding proteins could then direct the mRNAs for storage or degradation (Hentze, Castello, Schwarzl, & Preiss, 2018). In fact, several RNA binding proteins have been shown to control the fate of the different mRNAs in *T. cruzi* (Romagnoli, Holetz, Alves, & Goldenberg, 2020).

Specific changes in expression in trypomastigotes overexpressing eIF2α mutants also included increased surface gp90. Gp90 is GPI-anchored (Guther, Cardoso de Almeida, Yoshida, & Ferguson, 1992) and belongs to the sialidase family (Franco, Paranhos-Bacalla, Yamauchi, Yoshida, & Da Silveira, 1993) and it is mainly expressed in metacyclic-trypomastigotes (Araguth, Rodrigues, & Yoshida, 1988). Gp90 inhibits cell invasion by metacyclic forms (Malaga &

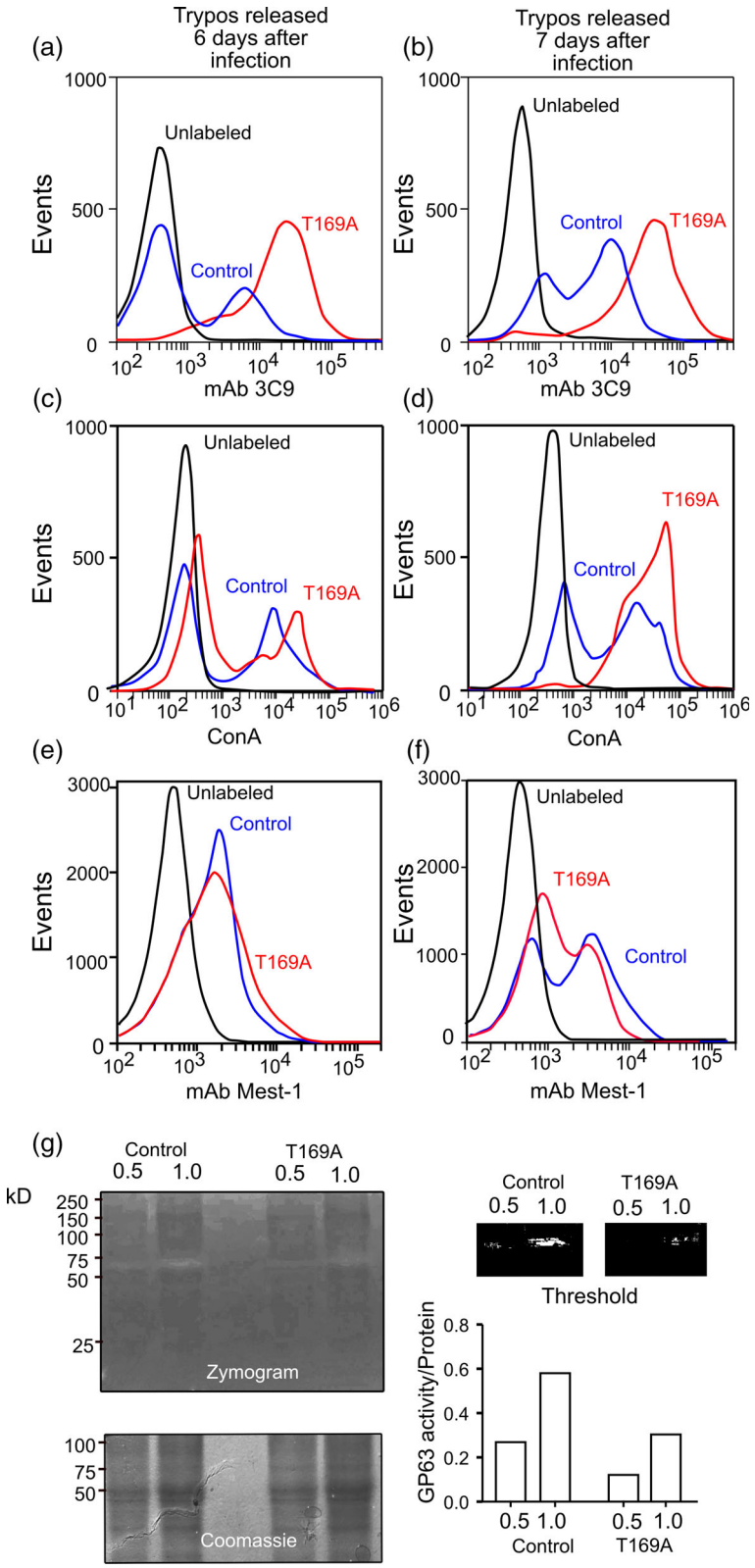

FIGURE 7 Effect of T169A replacement on the expression of surface proteins of trypomastigotes. Trypomastigotes obtained from infected U-2 OS cells at the sixth and seventh day of infection of control cell line (parasites containing the Cas9 gene, blue lines) and the parasite line in which eIF2α was replaced (Cas9-T169A, red lines) were labelled by mAb 3C9 (a and b) or Concanavalin A-biotin (c and d) and analysed by flow cytometry as described in Methods section. The black lines indicate the analysis of non-labelled parasites, which were identical for both lines. The figure shows one experiment representative of two independent experiments with similar results

Yoshida, 2001) by down-modulating lysosomal sequestration during parasite entry (Rodrigues, Sant'ana, Juliano, & Yoshida, 2017). Therefore, the presence of gp90 in trypomastigotes bearing the eIF2α mutants offers additional reason why, in the overexpressor lineages, we found infective parasites. However, mutation of endogenous eIF2α did not impact on gp90, suggesting that dysregulation due to eIF2α may require increased levels of the protein rather than simply loss of phospho-forms. Nevertheless, the phenotypes of both types of mutants are similar, with parasites becoming less infective and proliferative in mammalian cells. An excess of non-phosphorylatable eIF2α

could act to inhibit eIF2α-kinases, which are crucial in many parasites (Zhang, Joyce, Sullivan Jr., & Nussenzweig, 2013; da Silva Augusto et al., 2015; Rao, Meleppattu, & Pal, 2016), and in support of this model, we found increased eIF2α kinase in the Cas9 mutated cells which is potentially a compensatory mechanism. Significantly, non-phosphorylated eIF2α interacts more strongly with eIF2B (Bogorad et al., 2017), which recycles GDP-eIF2 to GTP-eIF2 necessary to form the trimeric complex and hence indicating that the mutant forms likely block the function of the entire complex.

In summary, we demonstrate that different developmental stages of *T. cruzi* are accompanied by changes in both overall levels of eIF2α and specific phosphorylation at threonine 169. The development of infective non-proliferative trypomastigotes that occurs in mammalian cells occurs in parallel to the phosphorylation of eIF2α followed by its decreased expression. When phosphorylation is prevented, the invasion and multiplication of intracellular parasites are reduced, most likely a consequence of altered translational activity before transformation in infective forms. Trypomastigotes shows low levels of eIF2α that remains unphosphorylated. Therefore, eIF2α phosphorylation is an addition level to regulate protein expression in *T. cruzi* especially during differentiation to infective forms of the parasite.

4 | EXPERIMENTAL PROCEDURES

The procedures used in this work were approved by the 'Comite de Ética em Pesquisa da Universidade Federal de São Paulo' under protocol 2666291015. All methods were performed in accordance with the relevant guidelines and regulations approved by the Universidade Federal de São Paulo.

4.1 | Parasites and cell cultures

Epimastigotes of *T. cruzi* (Y strain) were cultivated at 28°C in autoclaved in LIT (liver infusion tryptose) medium supplemented with 10 μg/ml hemin, 10% FBS, 2 mg/ml glucose, 59 mg/ml penicillin and 133 mg/ml streptomycin (Camargo, 1964). The parasites were diluted from 2×10^7 to 5×10^6 cells/ml to be kept in log phase growth. Epimastigotes overexpressing GFP fused to the *N*-terminal residue of histone H2b from *T. cruzi* (Ramirez et al., 2000) and overexpressing TceIF2α were both cultivated in the same medium with addition of 50 μg/ml of Geneticin/G418 (Thermo Fisher Scientific).

Metacyclic-trypomastigotes were obtained from exponentially growing epimastigotes cultures (1×10^7 parasites/ml) after 4x dilution in Grace's insect medium (Thermo Fisher Scientific) previously adjusted to pH 6.2 with 2 N HCl. Metacyclic-trypomastigotes appeared after 7 days at 28°C, and were purified by DEAE-cellulose columns (DE-52, Whatman) as described (Teixeira & Yoshida, 1986). For metacyclogenesis quantification, late log phase-cultured epimastigotes were centrifuged at 2,000 g for 10 min, washed once in TAU medium (190 mM NaCl, 17 mM KCl, 0.035%, $NaHCO_3$, 2 mM $CaCl_2$, 2 mM $MgCl_2$, 1.5 mM sodium phosphate, pH 6.5) and suspended to 1×10^9 parasites/ml in TAU medium. Parasites were incubated for 2 hr at 28°C, diluted 100x in TAU3AAG medium (TAU containing 10 mM glucose, 2 mM aspartic acid, 50 mM glutamic acid and 10 mM proline) and maintained in 75 cm^2 tissue culture flasks for 5 days at 28°C. The floating parasites were collected, attached to glass coverslips, fixed with 50% cold methanol and stained with Giemsa reagent previously diluted 1:4 in tap water. Optical microscopy was used to count and identify epimastigotes and metacyclic forms by evaluating the position of kinetoplast relative to the nucleus.

T. cruzi tissue-culture derived trypomastigotes were obtained from supernatants of LLC-MK2 cells (Rhesus monkey kidney epithelial cells, ATCC CCL-7) cultivated in low glucose Dulbecco's Modified Eagle Medium (DMEM, Thermo-Fischer Scientific) supplemented with 3.7 g/L sodium bicarbonate, 10% FBS, 59 mg/ml penicillin and 133 mg/ml streptomycin at 37°C in a 5% CO_2 atmosphere. Alternatively, U-2OS cells (Human osteosarcoma cells, Banco de Células do Rio de Janeiro) were used in the same conditions. The cells were infected with metacyclic-trypomastigotes, or with trypomastigotes released from infected cells. The parasites were collected by centrifugation at 1,500 g for 5 min, incubated for at least 60 min at 37°C and trypomastigote-enriched supernatants were collected and used for experiments.

Intracellular amastigotes were obtained from infected LLC-MK2 cells, first by removing the monolayer with trypsin, washing the cells in culture medium and suspending infected cells in 27 mM K_2HPO_4, 8 mM Na_2HPO_4 and 26 mM KH_2PO_4, pH 7.2. The cells were then lysed in a Potter-Elvehjem homogeniser, and free parasites were separated from cell debris by several rounds of centrifugation at 800 g for 2–5 min, before collecting the purified amastigotes by centrifugation at 2,000 g for 5 min (Abuin et al., 1999).

4.2 | Parasite invasion and intracellular replication

To evaluate the progression of *T. cruzi* infection inside the mammalian cell, LLC-MK2 (or U-2OS) cells were seeded onto 13 mm glass coverslips in 24-well plates and incubated at 37°C. The next day, 5×10^5 trypomastigotes from each lineage was diluted in 500 μl of culture medium and added to each well for incubation for 2 hr. The wells were washed twice with PBS and the incubation continued for 2, 3 and 4 days. The coverslips were fixed in Bouin solution (5% acetic acid, 9% formaldehyde and 0.9% picric acid) for 5 min and washed four or five times with PBS before staining for 1 hr with Giemsa solution (previously diluted 1:10 in tap water and filtered in Whatman 2 paper). Glass coverslips were dehydrated in acetone, acetone with xylol and only xylol before mounted in glass slides covered with Entellan mounting medium (Sigma-Aldrich). Coverslips were visualised under an optical microscope and the number of intracellular amastigotes was assessed in 100 infected cells.

Alternatively, we employed a high content analysis of infection using U-2 OS human bone osteosarcoma cells, also maintained in low glucose DMEM and 10% FBS. Two thousand cells were suspended in 100 μl medium, or 800 cells in 40 μl, then seeded in 96- or 384-well

black plates with clear bottom (Greiner Bio-One) respectively. After 16–24 hr at 37°C, 50 μl or 10 μl of a trypomastigote suspension in DMEM, containing the indicated concentrations of parasites obtained from infected cells were added, respectively, to the 96- or 384-well plates. Two, three or four days, after the infection, the cells were fixed with 4% PFA (paraformaldehyde) in PBS, stained with Draq5 (Biostatus) in the dark and at room temperature for 30 min.

The plates were then imaged by using a High Content Imaging System INCell (GE) at 20X magnification. Six images were acquired per well with thousands of cells per image. Images were analysed with the High Content Analysis (HCA) software Investigator version 1.6 (GE) for identification, segmentation and quantification of host cell nucleus, cytoplasm and intracellular parasites. The HCA provided output data for all images as the total number of cells, total number of infected cells and the total number of intracellular parasites. The ratio of infected cells to the total number of cells was calculated and defined as the Infection Ratio for invasion assays and the mean number of amastigotes per infected cell was also calculated for replication assays.

4.3 | T. cruzi eIF2α constructions for overexpression

The coding gene of *T. cruzi* eIF2α was amplified from genomic DNA of DM28c strain (TCDM_00323, http://tritrypdb.org) and inserted on pDONR221 (Thermo Fischer Scientific) Gateway vector before transferring to pDEST17 vector, as described previously (Tonelli et al., 2011). The substitution of serine 43 to alanine (S43A) was realised by two-step PCR, initially generating fragments using PfuI polymerase (Thermo Fisher Scientific) and the primers TceIF2FX and TceIF2Rbg and eifSA and eIF2RH. All primer sequences are listed in Table S1. Both fragments were gel purified and used as templates for the second PCR with TceIF2FX and eIF2RH to amplify the full version of TceIF2α containing the mutated S43A. The substitution of the phosphorylation site at threonine 169 to alanine (T169A) was performed similarly, firstly utilising the primers TceIF2 FX and eIF2T169ARev or eIF2T169AFow and eIF2RH, followed by a second PCR reaction to amplify a full version of TceIF2α containing the mutated T169A using TceIF2FX and eIF2RH. To obtain a double mutant (S43A/T169A), the TceIF2α gene with mutated S43A was used as template for both PCR reactions employed to generate the T169A construct. The full length fragments were digested with EcoRI and HindIII and inserted on p33 vector (Ramirez et al., 2000) previously digested with the same enzymes. The presence of the expected mutations was confirmed by sequencing reactions using primers p33SeqFow2 and eIF2RH.

To obtain parasite strains expressing modified eIF2α, 4×10^7 epimastigotes were washed in 137 mM NaCl, 21 mM Hepes pH 7.0, 5.5 mM Na_2HPO_4, 5 mM KCl and 0.77 mM glucose and incubated with 15 μg of circular plasmids diluted in the same buffer. The mixtures were submitted to electric pulses using 0.4 cm cuvettes in the Amaxa Nucleofactor (Lonza) set at program U-33 at room temperature. Pulsed parasites were then diluted in 5 ml of LIT medium containing 10% de FBS and after 24 hr Geneticin-G418 (Thermo Fisher Scientific) was added to 500 μg/ml to obtain stable transformants. Chromosomal and episomal DNA were obtained from selected parasites, as described before (Medina-Acosta & Cross, 1993), and submitted to sequencing reaction using the primer p33SeqFow2.

4.4 | Generation of T169A replacement

The parasites of Y strain expressing Cas9 were generated by transfection with plasmid pTREX-Cas9-Neo (Lander, Li, Niyogi, & Docampo, 2015), selected and maintained in the same medium supplemented with 200 μg/ml Geneticin G418. For transfection, 4×10^7 exponentially growing Cas9 epimastigotes were collected and centrifuged at 2,000 g for 5 min, parasites were washed in 1 ml of electroporation buffer (5 mM KCl, 0.15 mM $CaCl_2$, 90 mM Na_2HPO_4, 50 mM HEPES, 50 mM Mannitol) (Pacheco-Lugo et al., 2017) and resuspended in 100 μl of electroporation buffer, along with 50 μl containing 2 μg of purified sgRNA and 1 μmol of the donor sequence. The sgRNA was generated by PCR using the oligonucleotide sgeIF2 (positions 578–597 of the eIF2α ORF) and the common primer that recognises the plasmid pUC sgRNA (Lander et al., 2015). The sgRNA was prepared by in vitro transcription using the MEGAShortscript Kit (Thermo Fisher Scientific) according to the manufacturer instructions and purified by phenol/chloroform extraction and ethanol precipitation. The donor DNA was the oligonucleotide eIF2T169don designed to replace the Thr 169 and contains a BssHII site. Parasites were transfected in 2 mm cuvettes using AMAXA Nucleofactor II electroporator, with two pulses of X-014 program. Subsequently, parasites were transferred to bottles with fresh LIT medium supplemented with 10% fetal bovine serum and maintained at 28°C for recovery. After 5 days, a new round of transfection was made. After the parasite recovery, the total DNA of the parasites was extracted and the region corresponding to eIF2α using the primers eIF2S43DFow and eIF2RH. The PCR products before and after 3 hr digestion with BssHII were analysed in 1% agarose gels in TAE buffer and ethidium bromide staining. Parasite clones were obtained by serial dilutions in 96 well plates in LIT medium.

4.5 | Western blotting

Parasites were collected by centrifugation at 2,000 g for 5 min and washed once in 10 mM Tris-HCl pH 7.5, 150 mM NaCl (TBS) containing phosphatase inhibitors (PhosStop, Sigma-Aldrich) and protease inhibitors (Complete, EDTA-free, Roche) as recommended by the manufactures. Cells were lysed by three cycles of freezing and thawing, centrifuged at 13,000 g for 10 min at 4°C and the supernatant containing the soluble proteins was collected. The amount of proteins was measured by Bradford assay (Bradford, 1976), mixed with SDS-PAGE sample buffer (Laemmli, 1970) and heated at 95°C for 5 min. Alternatively, total extracts were prepared from TBS-washed

parasites by suspending the pellets directly on sample buffer followed by heat denaturation. Electrophoresis was performed in polyacrylamide gels containing SDS and the proteins transferred to nitrocellulose membranes by standard procedures. The membranes were stained with 0.5% Ponceau S in 3% acetic acid, blocked with TBS containing 0.1% Tween 20 (TBS-T) and 5% BSA for 1–12 hr. For the TceIF2α phosphorylation analysis in intracellular parasites, the membranes were cut separating the portion containing proteins with mass above 40 and below 60 kDa. Membrane pieces were incubated for 2 hr with an affinity purified antibody that reacts with the phosphorylated T169 of TceIF2α (Tonelli et al., 2011) diluted in blocking buffer. The antibodies were re-purified by sequential affinity chromatography on peptides NH_3YTEI[^{P}T]RIRIRAIGKC-amide and NH_3YTEIRIRIRAIGKC-amide (GeneScript) both coupled to SulfoLink® Coupling Resin (Thermo Fisher Scientific). Elution from the first column was achieved by using 50 mM glycine pH 2.8 buffer, followed by neutralisation by adding 2 M Tris-HCl pH 9.0 and the second column was only used to adsorb non-phospho-specific antibodies. Anti-*T. cruzi* eIF2α antibodies that recognise the full protein was obtained by immunising mice with the *T. cruzi* recombinant protein cloned in pET28a and expressed in *Escherichia coli* BL21 as described previously (da Silva Augusto et al., 2015).

Membranes were washed three times in TBS-T for 10 min, incubated for 1 hr with anti-rabbit IgG peroxidase-conjugated antibody (Thermo Fischer Scientific) diluted 1:20,000 in TBS, and washed more three times in TBS-T for 10 min. Bound antibodies were detected by ECL (EMD Millipore) using an Odyssey Fc System (LI-COR Biosciences). The same membrane pieces were re-probed with an anti-TceIF2α serum from mice immunised with a recombinant *T. cruzi* eIF2α expressed in *E. coli* Bl21 using the pDEST17 vector and purification in Nickel-agarose column. The serum was diluted 1:2,000 in PBS containing 5% non-fat dry milk. After 1 hr incubation, the membranes were washed three times with TBS-T followed by 1 hr incubation with anti-mouse IgG IRDye 800 (LI-COR Biosciences) 1:10,000 in PBS. Membranes were washed three times with TBS-T and bound antibodies detected as described above. Other immunoblots were performed with rabbit serum anti-Hsp70 diluted 1:10,000 (McDowell, Ransom, & Bangs, 1998), rabbit serum anti-TceIF5A diluted 1:10,000 (Chung, Rocha, Tonelli, Castilho, & Schenkman, 2013), rabbit serum anti-BiP diluted 1:5,000 (Bangs, Uyetake, Brickman, Balber, & Boothroyd, 1993), mice ascites for anti-gp82 3F6 monoclonal diluted 1:100 (Araya et al., 1994) and mice ascites for anti-gp90 5E7 monoclonal diluted 1:100 (Franco et al., 1993). Anti-*T. brucei* aldolase was prepared by immunising rabbits with recombinant *T. brucei* aldolase, as described (Opperdoes & Borst, 1977), all diluted in blocking buffer and incubated for at least 1 hr and detected as described above. Pixel quantification was performed using Image Studio version 5.2 (LI-COR Biosciences).

4.6 | Zymogram analysis

Trypomastigotes obtained from infected U2-OS cells and stored at −80°C until use. The parasites (3×10^7) were then thawed in 60 μl of SDS-PAGE sample buffer without ß-mercaptoethanol and incubated with 1 μl Benzonase (Merck Millipore) and loaded in a 10% polyacrylamide gel containing 20 mg/ml gelatin. The electrophoresis was performed at 10 V/cm and at 4°C. The gel was then incubated for 1 hr in 2.5% Triton-X100 at 37°C and then in 50 mM Tris-HCl pH 7.5, 200 mM, NaCl, 5 mM $CaCl_2$ and 0.02% Brij-35 (vol/vol) for 12 hr before staining with Coomassie Blue R250 and destaining in water/ethanol/acetic acid (4/4/1).

4.7 | Parasite size quantification

Exponentially growing *T. cruzi* epimastigotes were collected by centrifugation at 2,000 g for 2 min, washed twice and suspended in PBS before addition to glass slides (Tekdon Inc) previously treated with 0.01% poly-L-lysine (Sigma-Aldrich). After 5 min, unattached cells were removed, and the slides were incubated with PFA for 15 min. The slides were washed twice with PBS and mounted with Prolong Gold Antifade Reagent (Thermo Fisher Scientific). Differential interference contrast images containing at least 100 parasites were acquired using an Orca R2 CCD camera (Hamamatsu) coupled to an Olympus BX-61 microscope equipped with a x100 pLan Apo-oil objective (NA 1.4) and the area of each parasite calculated after manually contouring each parasite using the Cell^M software (Olympus). Data were analysed by non-parametric two-way ANOVA with Graph Pad version 6.

4.8 | Flow cytometer analysis

Tissue culture-derived trypomastigotes were collected and washed by centrifugation (2,000 g, 5 min) and resuspended in PBS. The parasites were fixed by adding the same volume of a 4% *p*-formaldehyde in PBS, which were maintained at 4°C until use. The fixed parasites were washed by centrifugation (2,000 g, 5 min) in a swing buckle rotor twice with PBS and resuspended to 2×10^7/ml. One hundred microlitres of the culture supernatant of hybridoma mAb 3C9 (Andrews, Hong, Robbins, & Nussenzweig, 1987) diluted 5X, the ascitic fluid of mAb Mest-1 (Suzuki et al., 1997) diluted 100X in PBS, or Concanavalin-biotin (Sigma-Aldrich) diluted 100X was then added to 100 μl of the fixed parasite suspension. After 1 hr incubation at room temperature, the suspension was centrifuged, washed once and resuspended in 100 μl of PBS, before addition of the same volume of anti-mouse IgG-Alexa 488 (Thermo-Fisher Scientific) or Streptavidin-Phycoerythrin (BD Biosciences). The samples were then incubated 30 min, washed, resuspended in 250 μl of PBS and fixed with the same volume of 4% p-formaldehyde in PBS. The samples were then analysed in Accury C6 flow cytometer (BD Biosciences).

4.9 | Polysome profiling

At least 1×10^9 exponentially growing epimastigotes, before or after pre-incubation with TAU medium for 2 hr were treated with

100 μg/ml cycloheximide at 28°C for 10 min, followed by ice cooling for additional 10 min. The cells were then collected by centrifugation at 2,000 g for 5 min at 4°C, washed in ice-cold PBS containing the same concentration of cycloheximide and suspended in approximately 300 μl of ice-cold Buffer A (10 mM Tris-HCl, pH 7.4, 300 mM KCl, 10 mM $MgCl_2$, 1 mM dithiothreitol and 100 μg/ml cycloheximide). A drop of Triton X-100 was added to the lateral side of tube to reach 1% (wt/vol) and the tubes were repeatedly mixed by inversion for about 3–5 min. The lysates were centrifuged at 6,000 g for 3 min at 4°C and the supernatants were transferred to a new tube. Stocks of heparin at 100 mg/ml and NaCl at 5 M were added to 1 mg/ml and 150 mM respectively. Samples containing the equivalent of 10 absorbance units at 260 nm were then loaded on the top of a 7–47% sucrose gradient in Buffer A, prepared using a Gradient Master (Biocomp). The tubes were centrifuged at 250,000 g for 2.5 hr in a Beckman SW41 rotor at 4°C. The gradient was collected from the top by injecting the bottom with a continuous flow of 60% sucrose at 1 ml/min using an Econo Gradient Pump (Bio-Rad) and the fractions were monitored by reading the absorbance at 254 nm.

4.10 | Parasitemia and immunosuppression analysis

BALB/c female mice (8–10 weeks old) were obtained from the CEDEME animal facility at UNIFESP and were maintained under pathogen-free conditions in individually ventilated cages, experiencing a 12 hr light/dark cycle with access to food and water ad libitum. Trypomastigotes (5×10^5) from the indicated lineages were injected intraperitoneally in five animals per group. Blood parasitemia was quantified by counting motile parasites in 5 μl fresh blood drawn from lateral tail veins every 2 days starting on day 1. Forty days after infection, each animal received 100 mg of cyclophosphamide (Genuxal, Baxter) per kg of body weight every 3 days (Huyan, Lin, Gao, Chen, & Fan, 2011). The parasitemia was then verified every 3–5 days and animal survival was recorded daily.

4.11 | Proteomic analyses

For proteomic analysis, parasites were maintained in LIT-10% FBS up to 1×10^7 ml in five independent cultures at 28°C performed in different weeks. The parasites were collected by centrifugation at 2,000 g, 10 min, washed once in PBS and stored at −80°C. The samples containing 2×10^7 parasites resuspended, boiled in 20 μl of SDS-PAGE sample buffer containing 5 mM DTT and loaded in precast Novex Value 4–12% Tris-Glycine gels. The electrophoresis was performed in 50 mM MOPS-50 mM Tris Base, 3.5 mM SDS, 1 mM EDTA at 100 V for 10 min. The migration portion of each lane was cut, and the gel pieces were fixed for 10 min at room temperature in one volume of 40% ethanol, 10% acetic acid. The fixative was removed, and the fixation repeated twice more. The bands were kept frozen at −80°C until processing for mass spectrometry analysis. The gel slices were submitted to reductive alkylation and in gel tryptic digest using routine procedures. The eluted peptides were then analysed by liquid chromatography–tandem mass spectrometry ($LC\text{-}MS^2$) on a ultimate 3,000 nano rapid separation LC system (Dionex) coupled to a Q Exactive HF Hybrid Quadrupole-Orbitrap mass spectrometer (Thermo-Fisher Scientific). Spectra were processed using the intensity-based label-free quantification (LFQ) method of MaxQuant (Cox & Mann, 2008) searching the *T. cruzi* YC6 annotated protein database (release 46) from TriTrypDB (Aslett et al., 2010). Minimum peptide length was set at six amino acids, isoleucine and leucine were considered indistinguishable and false discovery rates (FDR) of 0.01 were calculated at the levels of peptides, proteins and modification sites based on the number of hits against the reversed sequence database. When the identified peptide sequence set of one protein contained the peptide set of another protein, these two proteins were assigned to the same protein group. The LFQ data were analysed using the Perseus software (Tyanova et al., 2016). A Student's *t* test comparing the control sample group to the respective modified strain generated $-\log_{10}$ *t*-test *p*-value plotted versus *t*-test difference to generate a volcano plot. Enrichment analysis was performed using a Fisher's exact test in Perseus with a Benjamin–Hochberg false discovery rate of 0.02. Proteomics data have been deposited to the ProteomeXchange Consortium via the PRIDE partner repository (Vizcaino et al., 2016) with the dataset identifier PXD018761.

4.12 | 5′UTR, μORF and IRES detection

The full genome of *T. cruzi* YC6 sequenced and annotated by Dr. Wei Wang and Prof. Rick Tarleton from the Centre for the Tropical & Emerging Global Diseases, University of Georgia was downloaded from https://tritrypdb.org/tritrypdb/ (Aslett et al., 2010) (version 46) and the RNAseq corresponding to the four parasite stages was kindly provided by Prof. Rick L. Tarleton and Dr. Wei Wang. The 5′UTR was obtained using the UTRme package (https://github.com/sradiouy/UTRme.git) using default parameters. μORFs were annotated as in (Radio et al., 2020). Briefly, open reading frames (ORF) in the 5′UTRs were obtained using the getORF tool (Rice, Longden, & Bleasby, 2000). μORFs in which the coding sequences start in the 5′UTR region and end within the main CDS (out of frame with respect to the main CDS AUG) were defined as overlapping μORFs (μORFo), whereas the ones contained entirely in the 5′UTR were defined as non-overlapping uORF (μORFno), in this case, the frame with respect to the main CDS AUG was not considered. Only μORFs with this characteristic were considered in the analysis: (a) AUG start codon; (b) at least 15 nucleotides from the μAUG to the 5′ end of the mRNA; (c) a maximum distance of 50 nucleotides between the stop codon of the μORF and the AUG of the main CDS; (d) minimum length of five amino acids. In the case of the μORFo, the requirements were: (a) start with AUG; (b) a minimum length of three amino acids before the AUG of the main CDS. The IRES sequence was predicted based on the best-score 5′UTR sequences, using IRESpy – Prediction of IRES by XGBoost (https://irespy.shinyapps.io/IRESpy). The data were

analysed and visualised using the Orange3 Data Mining (https://orange.biolab.si).

ACKNOWLEDGEMENTS

We would like to thank Dr. Leonardo Augusto Silva for preparing the S43A bacterial construct, Dra. Beatriz A. Castilho for stimulating discussions, Dr. Caio Haddad Franco for the help with the HCS experiments, Dra. Normanda Souza Melo for preparing the samples for proteomic analysis, Luiz Severino Silva for handling and counting parasite in mice, and Claudio Rogério Oliveira and Claudeci Medeiros da Costa for the general technical support in the laboratory. We deeply acknowledge Rick Tarleton and Wei Wang for providing us the RNA seq data and for releasing before publication the full genome of YC6 with annotations in Tritrypdb.org. This work was funded through grants from Fundação de Amparo à Pesquisa do Estado de São Paulo (FAPESP, 2015/20031-0), Conselho Nacional de Desenvolvimento Científico e Tecnológico (CNPq 445655/2014-3 and INCTV-CNPq to S.S). F.C.M. was supported by a FAPESP doctoral fellowship (2014/01577-2), A.M.M. by a FAPESP postdoctoral fellowship (2017/02496-4), and M.A.V.C. by an undergraduate fellowship from CNPq (PIBIC-Unifesp).

CONFLICT OF INTEREST

The authors declare no conflicts of interest.

AUTHOR CONTRIBUTION

Fabricio Castro Machado, performed the experiments shown in Figures 1, 2, 3a, 5a–d, 6, S1a,b,e,f, S2a, S3a,b, S6, and S7; Paula Bittencourt-Cunha, cloned and characterised the Cas9-T69A clone and performed the experiments shown in Figures 3b,c and 5e–h; Amaranta Muniz Malvezzi, generated the Cas9-T169 and Figures S2b and S3c; Mirella Árico helped to isolate the Cas9-T169 line and performed the experiments in Figures 3b, S1c, and S3c,d; Martin Zoltner performed bioinformatics analysis of the proteomic data that generated Figure 3d and Tables S2 and S3; Mark C. Field helped in planning the proteomic analysis; Santiago Radio calculated and analysed the μORF; Pablo Smircich provide the strategy to determine the 5′UTRs; Sergio Schenkman performed the experiments of Figure 7, gene identification and correlation analysis; Sergio Schenkman, Fabricio Castro Machado, Paula Bittencourt-Cunha, Amaranta Muniz Malvezzi, Pablo Smircich, Martin Zoltner and, Mark C. Field planed, analysed data and wrote the manuscript.

ORCID

Fabricio Castro Machado https://orcid.org/0000-0001-8658-8471
Paula Bittencourt-Cunha https://orcid.org/0000-0002-3913-1441
Amaranta Muniz Malvezzi https://orcid.org/0000-0003-4700-3316
Mirella Arico https://orcid.org/0000-0003-4905-3982
Santiago Radio https://orcid.org/0000-0001-5238-4956
Pablo Smircich https://orcid.org/0000-0002-3856-3920
Martin Zoltner https://orcid.org/0000-0002-0214-285X
Mark C. Field https://orcid.org/0000-0002-4866-2885
Sergio Schenkman https://orcid.org/0000-0001-9353-8480

REFERENCES

Abuin, G., Freitas, L., Colli, W., Alves, M., & Schenkman, S. (1999). Expression of trans-sialidase and 85-kDa glycoprotein genes in *Trypanosoma cruzi* is differentially regulated at the post-transcriptional level by labile protein factors. *The Journal of Biological Chemistry*, *274*, 13041–13047.

Amorim, J. C., Batista, M., da Cunha, E. S., Lucena, A. C. R., Lima, C. V. P., Sousa, K., … Marchini, F. K. (2017). Quantitative proteome and phosphoproteome analyses highlight the adherent population during *Trypanosoma cruzi* metacyclogenesis. *Scientific Reports*, *7*, 9899.

Andreev, D. E., O'Connor, P. B., Fahey, C., Kenny, E. M., Terenin, I. M., Dmitriev, S. E., … Baranov, P. V. (2015). Translation of 5′ leaders is pervasive in genes resistant to eIF2 repression. *eLife*, *4*, e03971.

Andrews, N. W., Hong, K. S., Robbins, E. S., & Nussenzweig, V. (1987). Stage-specific surface antigens expressed during the morphogenesis of vertebrate forms of *Trypanosoma cruzi*. *Experimental Parasitology*, *64*, 474–484.

Araguth, M. F., Rodrigues, M. M., & Yoshida, N. (1988). *Trypanosoma cruzi* metacyclic trypomastigotes: Neutralization by the stage-specific monoclonal antibody 1G7 and immunogenicity of 90 kD surface antigen. *Parasite Immunology*, *10*, 707–712.

Araya, J. E., Cano, M. I., Yoshida, N., & Da Silveira, J. F. (1994). Cloning and characterization of a gene for the stage-specific 82-kDa surface antigen of metacyclic trypomastigoates of *Trypanosoma cruzi*. *Molecular and Biochemical Parasitology*, *65*, 161–169.

Aslett, M., Aurrecoechea, C., Berriman, M., Brestelli, J., Brunk, B. P., Carrington, M., … Wang, H. (2010). TriTrypDB: A functional genomic resource for the Trypanosomatidae. *Nucleic Acids Research*, *38*, D457–D462.

Aulas, A., Fay, M. M., Lyons, S. M., Achorn, C. A., Kedersha, N., Anderson, P., & Ivanov, P. (2017). Stress-specific differences in assembly and composition of stress granules and related foci. *Journal of Cell Science*, *130*, 927–937.

Avila, A. R., Dallagiovanna, B., Yamada-Ogatta, S. F., Monteiro-Goes, V., Fragoso, S. P., Krieger, M. A., & Goldenberg, S. (2003). Stage-specific gene expression during *Trypanosoma cruzi* metacyclogenesis. *Genetics and Molecular Research*, *2*, 159–168.

Avila, C. C., Peacock, L., Machado, F. C., Gibson, W., Schenkman, S., Carrington, M., & Castilho, B. A. (2016). Phosphorylation of eIF2alpha on threonine 169 is not required for *Trypanosoma brucei* cell cycle arrest during differentiation. *Molecular and Biochemical Parasitology*, *205*, 16–21.

Baird, T. D., & Wek, R. C. (2012). Eukaryotic initiation factor 2 phosphorylation and translational control in metabolism. *Advances in Nutrition*, *3*, 307–321.

Bangs, J. D., Uyetake, L., Brickman, M. J., Balber, A. E., & Boothroyd, J. C. (1993). Molecular cloning and cellular localization of a BiP homologue in *Trypanosoma brucei*. Divergent ER retention signals in a lower eukaryote. *Journal of Cell Science*, *105*, 1101–1113.

Belew, A. T., Junqueira, C., Rodrigues-Luiz, G. F., Valente, B. M., Oliveira, A. E. R., Polidoro, R. B., … Teixeira, S. M. R. (2017). Comparative transcriptome profiling of virulent and non-virulent *Trypanosoma cruzi* underlines the role of surface proteins during infection. *PLoS Pathogens*, *13*, e1006767.

Bogorad, A. M., Lin, K. Y., & Marintchev, A. (2017). Novel mechanisms of eIF2B action and regulation by eIF2alpha phosphorylation. *Nucleic Acids Research*, *45*, 11962–11979.

Bradford, M. M. (1976). A rapid and sensitive method for the quantitation of microgram quantities of protein utilizing the principle of protein-dye binding. *Analytical Biochemistry*, *72*, 248–254.

Brecht, M., & Parsons, M. (1998). Changes in polysome profiles accompany trypanosome development. *Molecular and Biochemical Parasitology*, *97*, 189–198.

Camargo, E. P. (1964). Growth and differentiation in *Trypanosoma cruzi*. I. Origin of metacyclic trypanosomes in liquid media. *Revista do Instituto de Medicina Tropical de São Paulo*, *6*, 93–100.

Cassola, A. (2011). RNA granules living a post-transcriptional life: The trypanosomes' case. *Current Chemical Biology*, *5*, 108–117.

Chow, C., Cloutier, S., Dumas, C., Chou, M. N., & Papadopoulou, B. (2011). Promastigote to amastigote differentiation of *Leishmania* is markedly delayed in the absence of PERK eIF2alpha kinase-dependent eIF2alpha phosphorylation. *Cellular Microbiology*, *13*, 1059–1077.

Chung, J., Rocha, A. A., Tonelli, R. R., Castilho, B. A., & Schenkman, S. (2013). Eukaryotic initiation factor 5A dephosphorylation is required for translational arrest in stationary phase cells. *The Biochemical Journal*, *451*, 257–267.

Clayton, C. (2019). Regulation of gene expression in trypanosomatids: Living with polycistronic transcription. *Open Biology*, *9*, 190072.

Cloutier, S., Laverdiere, M., Chou, M.-N., Boilard, N., Chow, C., & Papadopoulou, B. (2012). Translational control through eIF2alpha phosphorylation during the *Leishmania* differentiation process. *PLoS One*, *7*, e35085.

Cox, J., & Mann, M. (2008). MaxQuant enables high peptide identification rates, individualized p.p.b.-range mass accuracies and proteome-wide protein quantification. *Nature Biotechnology*, *26*, 1367–1372.

Cribb, P., Esteban, L., Trochine, A., Girardini, J., & Serra, E. (2010). *Trypanosoma cruzi* TBP shows preference for C/G-rich DNA sequences in vitro. *Experimental Parasitology*, *124*, 346–349.

Cuevas, I. C., Cazzulo, J. J., & Sanchez, D. O. (2003). gp63 homologues in *Trypanosoma cruzi*: Surface antigens with metalloprotease activity and a possible role in host cell infection. *Infection and Immunity*, *71*, 5739–5749.

da Silva Augusto, L., Moretti, N. S., Ramos, T. C., de Jesus, T. C., Zhang, M., Castilho, B. A., & Schenkman, S. (2015). A membrane-bound eIF2 alpha kinase located in endosomes is regulated by heme and controls differentiation and ROS levels in *Trypanosoma cruzi*. *PLoS Pathogens*, *11*, e1004618.

Das, A., Morales, R., Banday, M., Garcia, S., Hao, L., Cross, G. A., … Bellofatto, V. (2012). The essential polysome-associated RNA-binding protein RBP42 targets mRNAs involved in *Trypanosoma brucei* energy metabolism. *RNA*, *18*, 1968–1983.

Elias, M., Marques-Porto, R., Freymuller, E., & Schenkman, S. (2001). Transcription rate modulation through the *Trypanosoma cruzi* life cycle occurs in parallel with changes in nuclear organisation. *Molecular and Biochemical Parasitology*, *112*, 79–90.

Ferreira, L. R., Dossin Fde, M., Ramos, T. C., Freymuller, E., & Schenkman, S. (2008). Active transcription and ultrastructural changes during *Trypanosoma cruzi* metacyclogenesis. *Anais da Academia Brasileira de Ciências*, *80*, 157–166.

Franco, F. R. S., Paranhos-Bacalla, G. S., Yamauchi, L. M., Yoshida, N., & Da Silveira, J. F. (1993). Characterization of a cDNA clone encoding the carboxy-terminal domain of a 90-kilodalton surface antigen of *Trypanosoma cruzi* metacyclic trypomastigotes. *Infection and Immunity*, *61*, 4196–4201.

Frevert, U., Schenkman, S., & Nussenzweig, V. (1992). Stage-specific expression and intracellular shedding of the cell surface trans-sialidase of *Trypanosoma cruzi*. *Infection and Immunity*, *60*, 2349–2360.

Fritz, M., Vanselow, J., Sauer, N., Lamer, S., Goos, C., Siegel, T. N., … Kramer, S. (2015). Novel insights into RNP granules by employing the trypanosome's microtubule skeleton as a molecular sieve. *Nucleic Acids Research*, *43*, 8013–8032.

Goldenberg, S., & Avila, A. R. (2011). Aspects of *Trypanosoma cruzi* stage differentiation. *Advances in Parasitology*, *75*, 285–305.

Guerra-Slompo, E. P., Probst, C. M., Pavoni, D. P., Goldenberg, S., Krieger, M. A., & Dallagiovanna, B. (2012). Molecular characterization of the *Trypanosoma cruzi* specific RNA binding protein TcRBP40 and its associated mRNAs. *Biochemical and Biophysical Research Communications*, *420*, 302–307.

Guther, M. L. S., Cardoso de Almeida, M. L., Yoshida, N., & Ferguson, M. A. J. (1992). Structural studies on the glycosylphosphadidylinositol membrane anchor of *Trypanosoma cruzi* 1G7-antigen. *The Journal of Biological Chemistry*, *267*, 6820–6828.

Haile, S., & Papadopoulou, B. (2007). Developmental regulation of gene expression in trypanosomatid parasitic protozoa. *Current Opinion in Microbiology*, *10*, 569–577.

Hentze, M. W., Castello, A., Schwarzl, T., & Preiss, T. (2018). A brave new world of RNA-binding proteins. *Nature Reviews. Molecular Cell Biology*, *19*, 327–341.

Hinnebusch, A. G. (2000). Mechanism and regulation of initiator methionyl-tRNA binding to ribosomes. In N. Sonenberg, J. W. B. Hershey, & M. B. Mathews (Eds.), *Translational control of gene expression* (pp. 185–243). Cold Spring Harbor, NY: Cold Spring Harbor Laboratory Press.

Huyan, X. H., Lin, Y. P., Gao, T., Chen, R. Y., & Fan, Y. M. (2011). Immunosuppressive effect of cyclophosphamide on white blood cells and lymphocyte subpopulations from peripheral blood of Balb/c mice. *International Immunopharmacology*, *11*, 1293–1297.

Jeacock, L., Faria, J., & Horn, D. (2018). Codon usage bias controls mRNA and protein abundance in trypanosomatids. *eLife*, *7*, e32496

Joyce, B. R., Queener, S. F., Wek, R. C., & Sullivan, W. J., Jr. (2010). Phosphorylation of eukaryotic initiation factor-2α promotes the extracellular survival of obligate intracellular parasite *Toxoplasma gondii*. *Proceedings of the National Academy of Sciences of the United States of America*, *107*, 17200–17205.

Kashiwagi, K., Takahashi, M., Nishimoto, M., Hiyama, T. B., Higo, T., Umehara, T., … Yokoyama, S. (2016). Crystal structure of eukaryotic translation initiation factor 2B. *Nature*, *531*, 122–125.

Kolev, N. G., Ramey-Butler, K., Cross, G. A., Ullu, E., & Tschudi, C. (2012). Developmental progression to infectivity in *Trypanosoma brucei* triggered by an RNA-binding protein. *Science*, *338*, 1352–1353.

Kramer, S. (2012). Developmental regulation of gene expression in the absence of transcriptional control: The case of kinetoplastids. *Molecular and Biochemical Parasitology*, *181*, 61–72.

Kramer, S., Queiroz, R., Ellis, L., Webb, H., Hoheisel, J. D., Clayton, C., & Carrington, M. (2008). Heat shock causes a decrease in polysomes and the appearance of stress granules in trypanosomes independently of eIF2α phosphorylation at Thr169. *Journal of Cell Science*, *121*, 3002–3014.

Krishnamoorthy, T., Pavitt, G. D., Zhang, F., Dever, T. E., & Hinnebusch, A. G. (2001). Tight binding of the phosphorylated alpha subunit of initiation factor 2 (eIF2alpha) to the regulatory subunits of guanine nucleotide exchange factor eIF2B is required for inhibition of translation initiation. *Molecular and Cellular Biology*, *21*, 5018–5030.

Kulkarni, M. M., Olson, C. L., Engman, D. M., & McGwire, B. S. (2009). *Trypanosoma cruzi* GP63 proteins undergo stage-specific differential posttranslational modification and are important for host cell infection. *Infection and Immunity*, *77*, 2193–2200.

Laemmli, U. K. (1970). Cleavage of structural proteins during the assembly of the head of bacteriophage T4. *Nature (London)*, *227*, 680–685.

Lahav, T., Sivam, D., Volpin, H., Ronen, M., Tsigankov, P., Green, A., … Myler, P. J. (2011). Multiple levels of gene regulation mediate differentiation of the intracellular pathogen *Leishmania*. *The FASEB Journal*, *25*, 515–525.

Lander, N., Li, Z. H., Niyogi, S., & Docampo, R. (2015). CRISPR/Cas9-induced disruption of Paraflagellar rod protein 1 and 2 genes in *Trypanosoma cruzi* reveals their role in Flagellar attachment. *MBio*, *6*, e01012.

Malaga, S., & Yoshida, N. (2001). Targeted reduction in expression of *Trypanosoma cruzi* surface glycoprotein gp90 increases parasite infectivity. *Infection and Immunity*, *69*, 353–359.

Markmiller, S., Soltanieh, S., Server, K. L., Mak, R., Jin, W., Fang, M. Y., … Yeo, G. W. (2018). Context-dependent and disease-specific diversity in protein interactions within stress granules. *Cell*, *172*, 590–604.e513.

Martinez-Calvillo, S., Vizuet-de-Rueda, J.C., Florencio-Martinez, L.E., Manning-Cela, R.G., & Figueroa-Angulo, E.E. (2010). Gene expression

in trypanosomatid parasites. *Journal of Biomedicine & Biotechnology*, *2010*, 525241.

McDowell, M. A., Ransom, D. M., & Bangs, J. D. (1998). Glycosylphosphatidylinositol-dependent secretory transport in *Trypanosoma brucei*. *The Biochemical Journal*, *335*, 681–689.

Medina-Acosta, E., & Cross, G. A. M. (1993). Rapid isolation of DNA from trypanosomatid protozoa using a simple 'mini-prep' procedure. *Molecular and Biochemical Parasitology*, *59*, 327–330.

Moon, S., Siqueira-Neto, J. L., Moraes, C. B., Yang, G., Kang, M., Freitas-Junior, L. H., & Hansen, M. A. (2014). An image-based algorithm for precise and accurate high throughput assessment of drug activity against the human parasite *Trypanosoma cruzi*. *PLoS One*, *9*, e87188.

Moraes, M. C., Jesus, T. C., Hashimoto, N. N., Dey, M., Schwartz, K. J., Alves, V. S., … Castilho, B. A. (2007). Novel membrane-bound eIF2alpha kinase in the flagellar pocket of *Trypanosoma brucei*. *Eukaryotic Cell*, *6*, 1979–1991.

Moretti, N. S., & Schenkman, S. (2013). Chromatin modifications in trypanosomes due to stress. *Cellular Microbiology*, *15*, 709–717.

Mucci, J., Lantos, A. B., Buscaglia, C. A., Leguizamon, M. S., & Campetella, O. (2016). The *Trypanosoma cruzi* surface, a nanoscale patchwork quilt. *Trends in Parasitology*, *33*, 102–112.

Mugo, E., & Clayton, C. (2017). Expression of the RNA-binding protein RBP10 promotes the bloodstream-form differentiation state in *Trypanosoma brucei*. *PLoS Pathogens*, *13*, e1006560.

Opperdoes, F. R., & Borst, P. (1977). Localization of nine glycolytic enzymes in a microbody-like organelle in *Trypanosoma brucei*: The glycosome. *FEBS Letters*, *80*, 360–364.

Pacheco-Lugo, L., Díaz-Olmos, Y., Sáenz-García, J., Probst, C. M., & DaRocha, W. D. (2017). Effective gene delivery to *Trypanosoma cruzi* epimastigotes through nucleofection. *Parasitology International*, *66*(3), 236–239.

Palam, L. R., Baird, T. D., & Wek, R. C. (2011). Phosphorylation of eIF2 facilitates ribosomal bypass of an inhibitory upstream ORF to enhance CHOP translation. *The Journal of Biological Chemistry*, *286*, 10939–10949.

Palenchar, J. B., & Bellofatto, V. (2006). Gene transcription in trypanosomes. *Molecular and Biochemical Parasitology*, *146*, 135–141.

Pavitt, G. D., Ramaiah, K. V., Kimball, S. R., & Hinnebusch, A. G. (1998). eIF2 independently binds two distinct eIF2B subcomplexes that catalyze and regulate guanine-nucleotide exchange. *Genes & Development*, *12*, 514–526.

Pereira, M., Malvezzi, A. M., Nascimento, L. M., da Costa Lima, T. D., Alves, V. S., Palma, M. L., … de Melo Neto, O. P. (2013). The eIF4E subunits of two distinct trypanosomatid eIF4F complexes are subjected to differential post-translational modifications associated to distinct growth phases in culture. *Molecular and Biochemical Parasitology*, *190*, 82–86.

Perez-Diaz, L., Correa, A., Moretao, M. P., Goldenberg, S., Dallagiovanna, B., & Garat, B. (2012). The overexpression of the trypanosomatid-exclusive TcRBP19 RNA-binding protein affects cellular infection by *Trypanosoma cruzi*. *Memórias do Instituto Oswaldo Cruz*, *107*, 1076–1079.

Piacenza, L., Alvarez, M. N., Peluffo, G., & Radi, R. (2009). Fighting the oxidative assault: The *Trypanosoma cruzi* journey to infection. *Current Opinion in Microbiology*, *12*, 415–421.

Radio, S., Fort, R. S., Garat, B., Sotelo-Silveira, J., & Smircich, P. (2018). UTRme: A scoring-based tool to annotate untranslated regions in Trypanosomatid genomes. *Frontiers in Genetics*, *9*, 671.

Radío, S., Garat, B., Sotelo-Silveira, J., & Smircich, P. (2020). Upstream ORFs influence translation efficiency in the parasite *Trypanosoma cruzi*. *Frontiers in Genetics*, *11*, 166.

Ramirez, M. I., Yamauchi, L. M., de Freitas, L. H., Jr., Uemura, H., & Schenkman, S. (2000). The use of the green fluorescent protein to monitor and improve transfection in *Trypanosoma cruzi*. *Molecular and Biochemical Parasitology*, *111*, 235–240.

Rao, S. J., Meleppattu, S., & Pal, J. K. (2016). A GCN2-like eIF2alpha kinase (LdeK1) of *Leishmania donovani* and its possible role in stress response. *PLoS One*, *11*, e0156032.

Rice, P., Longden, I., & Bleasby, A. (2000). EMBOSS: The European molecular biology open software suite. *Trends in Genetics*, *16*, 276–277.

Rodrigues, J. P. F., Sant'ana, G. H. T., Juliano, M. A., & Yoshida, N. (2017). Inhibition of host cell lysosome spreading by *Trypanosoma cruzi* Metacyclic stage-specific surface molecule gp90 downregulates parasite invasion. *Infection and Immunity*, *85*(9), e00302-17

Romagnoli, B. A. A., Holetz, F. B., Alves, L. R., & Goldenberg, S. (2020). RNA binding proteins and gene expression regulation in *Trypanosoma cruzi*. *Frontiers in Cellular and Infection Microbiology*, *10*, 56.

Rubin-de-Celis, S. S., Uemura, H., Yoshida, N., & Schenkman, S. (2006). Expression of trypomastigote trans-sialidase in metacyclic forms of *Trypanosoma cruzi* increases parasite escape from its parasitophorous vacuole. *Cellular Microbiology*, *8*, 1888–1898.

Schuller, A. P., Wu, C. C., Dever, T. E., Buskirk, A. R., & Green, R. (2017). eIF5A functions globally in translation elongation and termination. *Molecular Cell*, *66*, 194–205 e195.

Schwede, A., Kramer, S., & Carrington, M. (2012). How do trypanosomes change gene expression in response to the environment? *Protoplasma*, *249*, 223–238.

Smircich, P., Eastman, G., Bispo, S., Duhagon, M. A., Guerra-Slompo, E. P., Garat, B., … Sotelo-Silveira, J. R. (2015). Ribosome profiling reveals translation control as a key mechanism generating differential gene expression in *Trypanosoma cruzi*. *BMC Genomics*, *16*, 443.

Sonenberg, N., & Hinnebusch, A. (2009). Regulation of translation initiation in eukaryotes: Mechanisms and biological targets. *Cell*, *136*, 731–745.

Souza, W. (2009). Structural organization of *Trypanosoma cruzi*. *Memórias do Instituto Oswaldo Cruz*, *104*(Suppl 1), 89–100.

Suzuki, E., Tanaka, A. K., Toledo, M. S., Takahashi, H. K., & Straus, A. H. (2002). Role of beta-D-galactofuranose in *Leishmania major* macrophage invasion. *Infection and Immunity*, *70*, 6592–6596.

Suzuki, E., Toledo, M. S., Takahashi, H. K., & Straus, A. H. (1997). A monoclonal antibody directed to terminal residue of beta-galactofuranose of a glycolipid antigen isolated from *Paracoccidioides brasiliensis*: Cross-reactivity with *Leishmania major* and *Trypanosoma cruzi*. *Glycobiology*, *7*, 463–468.

Teixeira, M. M. G., & Yoshida, N. (1986). Stage-specific surface antigens of metacyclic trypomastigotes of *Trypanosoma cruzi* identified by monoclonal antibodies. *Molecular and Biochemical Parasitology*, *18*, 271–282.

Tonelli, R. R., Augusto, L.d. S., Castilho, B. A., & Schenkman, S. (2011). Protein synthesis attenuation by phosphorylation of eIF2alpha is required for the differentiation of *Trypanosoma cruzi* into infective forms. *PLoS One*, *6*, e27094.

Tyanova, S., Temu, T., Sinitcyn, P., Carlson, A., Hein, M. Y., Geiger, T., … Cox, J. (2016). The Perseus computational platform for comprehensive analysis of (prote)omics data. *Nature Methods*, *13*, 731–740.

Umaer, K., & Williams, N. (2015). Kinetoplastid specific RNA-protein interactions in *Trypanosoma cruzi* ribosome biogenesis. *PLoS One*, *10*, e0131323.

Vizcaino, J. A., Csordas, A., Del-Toro, N., Dianes, J. A., Griss, J., Lavidas, I., … Hermjakob, H. (2016). 2016 update of the PRIDE database and its related tools. *Nucleic Acids Research*, *44*, 11033.

Yoshida, N., Blanco, S. A., Araguth, M. F., Russo, M., & Gonzalez, J. (1990). The stage-specific 90-kilodalton surface antigen of metacyclic trypomastigotes of *Trypanosoma cruzi*. *Molecular and Biochemical Parasitology*, *39*, 39–46.

Zhang, M., Joyce, B. R., Sullivan, W. J., Jr., & Nussenzweig, V. (2013). Translational control in *Plasmodium* and *Toxoplasma* parasites. *Eukaryotic Cell*, *12*, 161–167.

Zinoviev, A., & Shapira, M. (2012). Evolutionary conservation and diversification of the translation initiation apparatus in trypanosomatids. *Comparative and Functional Genomics*, *2012*, 813718.

SUPPORTING INFORMATION

Additional supporting information may be found online in the Supporting Information section at the end of this article.

How to cite this article: Castro Machado F, Bittencourt-Cunha P, Malvezzi AM, et al. EIF2α phosphorylation is regulated in intracellular amastigotes for the generation of infective *Trypanosoma cruzi* trypomastigote forms. *Cellular Microbiology*. 2020;e13243. https://doi.org/10.1111/cmi.13243